Fundamental Studies of Reactive Intermediates in Organometallic Chemistry

Thesis by

Amy Elizabeth Stevens

In Partial Fulfillment of the Requirements

for the Degree of

Doctor of Philosophy

California Institute of Technology

Pasadena, California

1981

(Submitted October 2, 1980)

ACKNOWLEDGMENTS

I thank J. L. Beauchamp for his patience not only in teaching me chemistry, but also in teaching me how to approach research.

W. A. Goddard and J. E. Bercaw have served on my committee and provided stimulating discussion over the past several years.

I was fortunate in being able to teach with Jack Beauchamp and Bill Goddard, from which experiences I learned a great deal.

D. Wayne Berman patched the photoionization mass spectrometer together one last time and assisted with the experiments given in Chapter IV.

Henriette Wymar deserves special thanks for her superb last-minute typing of this thesis. Emily Olsen and Virginia Umland typed some portions.

I thank the National Science Foundation for a Graduate Fellowship, and the California Institute of Technology for financial support.

Abstract

The techniques of ion cyclotron resonance spectroscopy and photoionization-mass spectrometry are used to characterize the thermochemistry and reactivity of transition metal and organometallic species in the gas-phase. Chapter I gives an introduction emphasizing the need for physical studies of these compounds. An assessment of the differences in chemical properties and reactivity between the gas phase and solution is also made.

Chapter II details the properties and reactions of $(CO)_5MnR$ ($R = H$, CH_3) determined using the techniques of ion cyclotron resonance spectroscopy. An examination of the products $(CO)_5Mn(R)H^+$, $(CO)_4Mn(R)H^+$, and $(CO)_5Mn^+$ which result from proton transfer with varying exothermicity to $(CO)_5MnR$ permits several thermochemical and mechanistic inferences. In particular the proton affinities of these species are derived and the mechanism of reductive elimination of RH from the conjugate acids is detailed.

An examination of processes involving negative ions yields the heterolytic bond energies $D[(CO)_5Mn^- - R^+]$. The hydride is found to be an exceptionally strong acid in the gas phase.

Positive and negative ion mass spectra and ion-molecule reactions are reported briefly.

Chapter III presents the results of an ion cyclotron-resonance trapped ion study of the kinetics of proton transfer from MnH^+ (formed as a fragment ion from $HMn(CO)_5$ by electron impact) to bases of varying strength. Deprotonation is rapid with bases whose proton

affinity exceeds 196 ± 3 kcal mol^{-1}. Using this value for PA[Mn] yields the homolytic bond dissociation energy $D[Mn^{+}\text{-}H]$ = 53 ± 3 kcal mol^{-1}.

In Chapter IV the results of a photoionization mass-spectrometric determination of the ionization potentials and selected fragment ion appearance potentials of $(CO)_5MnR$ where R = H, CH_3, CH_2F, CHF_2 and CF_3 are presented. A comparison of the appearance potential of $(CO)_5Mn^{+}$ from all five species yields the metal-carbon bond dissociation energies relative to the metal-hydrogen bond dissociation energy with no additional thermochemical data. Using the literature value $D^{0}[(CO)_5Mn\text{-}H]$ = 57 kcal/mol gives $D^{0}[(CO)_5Mn\text{-}R]$ = 44, 32, 33, and 42 kcal/mol, respectively. Fragmentation thresholds for the metal carbene fragment ions $(CO)_5MnCXY^{+}$ where X, Y = H or F are analyzed to yield the fluoride and hydride affinities of these species. Ion cyclotron resonance spectroscopy is used to examine hydride and fluoride transfer reactions involving these carbenes to corroborate the photoionization data. The carbene bond dissociation energies $D^{0}[(CO)_5Mn^{+}\text{-}CXY]$ decrease from 104 to 98 to 82 kcal/mol with successive substitution of F for H.

In Chapter V the proton affinities of twenty organotransition metal complexes in the gas phase are reported. Combined with adiabatic ionization potentials, these data yield metal-hydrogen homolytic bond energies for the sixteen species for which protonation occurs on the metal center. These bond energies range from 53 to 87 kcal/mol. Bond energies increase on going from a first-row

complex to its second-row homologue, but no increase is seen on going to the third-row metal. The metal-hydrogen bond energy decreases markedly with increasing oxidation state of the same metal. Comparison to isoelectronic neutral complexes is made.

TABLE OF CONTENTS

Chapter I

Introduction

Introduction

Interest in the physical chemistry of organometallic complexes is very recent, with essentially all of the work in this field being reported within the last several years. One major cause of this change, "the energy crisis", has consequences extending beyond the realm of the chemical world, needless to say. In chemistry, however, its effect has been to promote intense interest in synthetic fuel production, efficient catalytic processes, hydrogen production and storage, and the utilization of solar energy.

Effective design of systems mentioned above would be greatly enhanced by a detailed knowledge of the mechanisms of processes effected by organometallic complexes. This is a considerably greater problem than it might first appear. Identification of reaction intermediates is difficult at best; their fleeting existence makes even spectroscopic characterization oftentimes impossible. Additionally, solvent molecules can be important participants in a reaction, not only in solvation of reactants or products, but sometimes acting as a ligand. In many instances several low-energy processes are competitive; the selectivity of a catalyst or reagent is very poor. Finally, there are very few quantitative data on bond strengths and acid-base properties of organometallic complexes, and only a limited number on activation parameters.

All too often the physical chemist's approach to organometallic complexes has been to place such fragile complexes as $(CO)_5Fe$[1-2] and $(\eta^6\text{-}C_6H_6)_2Cr$[3] in a high-powered laser beam and note that metal atoms are produced. However, several very elegant studies of organometallic

complexes have been reported. Notable among these is a study of the decomposition of $(CO)_5Fe$ promoted by the SF_6 absorption of pulsed CO_2 infrared laser radiation, from which the bond energy $D[(CO)_4Fe\text{-}CO]$ = 49 ± 3 kcal/mol is determined.[4] Laser photoelectron spectrometry of the negative ions of iron and iron carbonyls had been used to determine the electron affinities of $Fe(CO)_n$, n = 0-4.[5] These data also provide information on the carbonyl vibrational modes and iron-carbonyl bond strengths in these species. The photodissociation of $Mn_2(CO)_{10}$ and $Re_2(CO)_{10}$ has been examined in a molecular beam.[6] These experiments clearly indicate the photoabsorption involves a parallel transition which results (within several picoseconds) only in metal-metal bond cleavage. This is taken as strong evidence for the photoabsorption to be the $\sigma \rightarrow \sigma^*$ transition of the metal-metal bond. $(CO)_4CoH$ has been investigated using matrix isolation techniques, and some spectroscopic evidence presented for identification of intermediates in the hydroformylation reaction.[7] Finally, ion-beam[8] and ion cyclotron resonance[9-12] studies of the reactions and thermochemistry of transition metal complexes and atomic ions are reported.

The work detailed in this thesis provides unique information on the gas-phase properties and reactions of organometallic complexes.

An assessment of the differences of the gas-phase to solution-phase chemistry is in order. One example is afforded by a discussion of the acidity of $(CO)_5MnH$. In the gas phase $(CO)_5MnH$ is found to be an exceptionally strong acid, with $D[(CO)_5Mn^-\text{-}H^+]$ = 318 ± 3 kcal/mol making the acidity comparable to that of HI and HBr. By contrast, $(CO)_5MnH$ in aqueous solution is only weakly acidic, with a pk_a = 7.1.[13]

This difference is attributed to the very poor solvation of $(CO)_5Mn^-$. These data can be used to estimate[14] the radius of $(CO)_5Mn^-$ to be about 3 Å; this is in reasonable agreement with the crystal structure of this anion.[15]

We have also determined the gas-phase acidities $D[(CO)_4Co^-H^+] \leq 313.6$ kcal/mol and $D[(CO)_4FeH^-H^+] = 328 \pm 5$ kcal/mol. The pk_a of these complexes are < 2 and 4.4, respectively.[16] $(CO)_4CoH$ is more acidic than $(CO)_5MnH$ in the gas phase, as would be predicted from the pk_a measurements, but $(CO)_4FeH_2$ is not. We interpret this as an indication of different solvation effects for $(CO)_4FeH_2$ and $(CO)_4FeH^-$ than are observed for the manganese and cobalt complexes.

A second example is made by comparison of the chemistry of several cyclopentadienyl iron complexes. Jolly and Pettit[17] report the attempted preparation of $(\eta^5\text{-}C_5H_5)Fe(CO)_2(CH_2)^+BF_4^-$ by cleavage of the ether $CpFe(CO)_2CH_2OCH_3$ with HBF_4. While the cationic complex could not be isolated, its presence was postulated to account for methylene transfer to produce norcarane from cyclohexene, and cis- and trans-1,2-dimethylcyclopropane from cis- and trans-2-butene, respectively. In the absence of olefins, $CpFe(CO)_2CH_3$ was isolated.

Protonation reactions of $CpFe(CO)_2CH_2OCH_3$ have also been utilized as a synthetic means to prepare a variety of $CpFe(CO)_2CH_2X$ derivatives.[18] Recently $CpFe(CO)_2CH_2S(CH_3)_2^+BF_4^-$ was prepared by similar techniques.[19] The sulphur ligand "stabilizes" the carbene complex; the salt is an isolable and easily handled reagent for the cyclopropanation of olefins.

The ion $CpFe(CO)_2CH_2^+$ is readily formed in the gas-phase, using the techniques of ion cyclotron resonance spectroscopy as given by reaction 1, in which $BH^+ = NH_4^+$, $C_2H_5^+$, CH_5^+, and H_3^+.[11]

$$CpFe(CO)_2CH_2OCH_3 + BH^+ \rightarrow CpFe(CO)_2CH_2^+ + CH_3OH + B\,. \qquad (1)$$

This ion undergoes several interesting reactions, for example, the carbene $CpFe(CO)_2(CHOCH_3)^+$ is produced at longer times or higher pressures, reaction 2.

$$CpFe(CO)_2CH_2^+ + CpFe(CO)_2CH_2OCH_3 \rightarrow$$

$$CpFe(CO)_2CH_3 + CpFe(CO)_2CHOCH_3^+ \qquad (2)$$

Addition of cyclohexene results in the production of $CpFe(CO)_2^+$ from the carbene; by analogy to the solution chemistry, this is attributed to reaction 3.

$CpFe(CO)_2CH_2^+ +$  $\rightarrow CpFe(CO)_2^+ +$ 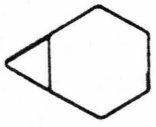 (3)

Each of the bases NH_3, CH_3CN, and CD_3CDO adds to the carbene, reaction 4.

$$CpFe(CO)_2CH_2^+ + B \rightarrow CpFe(CO)_2CH_2\text{-}B^+ \qquad (4)$$

As is detailed above, the reactions of $CpFe(CO)_2CH_2^+$ in the gas phase, specifically methylene transfer to cyclohexene, hydride abstraction to yield $CpFe(CO)_2CH_3$, and addition of n-donor bases to the methylene carbon, are entirely in accord with the reactions of this species in solution. Further, the reactions of $CpRe(PPh_3)(NO)(CHR)^+$

($R = H$, OCH_3, and OH) in solution[20] have provided an excellent demonstration of completely analogous reactivity to that of $CpFe(CO)_2CH_2^+$.

The results presented in this thesis provide not only thermochemical and mechanistic information of gas-phase species, but provide some interesting chemistry which complements solution-phase studies.

References

1. Karny, Z.; Naaman, R.; Zare, R. N. Chem. Phys. Lett. 1978, 59, 33.
2. Yardly, J. T.; Rosan, A.; Gitlin, B.; Nathanson, G., Proceedings, Symposium on Laser Photochemistry in Large Molecules and Solids, San Jose, California, Aug. 20-22, 1980.
3. Fisanick, G. J.; Robin, M. B.; Eichelberger, IV, T. S.; Kuebler, N. Proceedings, Symposium on Laser Photochemistry in Large Molecules and Solids, San Jose, California, Aug. 20-22, 1980.
4. Smith, G. P., Abstracts of the Second Chemical Conference of the North American Continent, Las Vegas, Nevada, Aug. 25-29, 1980.
5. Engelking, P. C.; Lineberger, W. C. J. Am. Chem. Soc. 1979, 101, 5569.
6. Freedman, A.; Bersohn, R. J. Am. Chem. Soc. 1978, 100, 4116.
7. Wermer, P.; Ault, B. S.; Orchin, M. J. Organomet. Chem. 1978, 162, 189.
8. Armentrout, P. B.; Beauchamp, J. L., J. Am. Chem. Soc. 1980, 102, 1736. Armentrout, P. B.; Beauchamp, J. L., Chem. Phys. 1980, 50, 37.
9. Allison, J.; Ridge, D. P. J. Am. Chem. Soc. 1979, 101, 4998, and references therein.
10. Beauchamp, J. L.; Stevens, A. E.; Corderman, R. R. Pure and Appl. Chem., 1979, 51, 967, and references therein.

References (continued)

11. Stevens, A. E.; Beauchamp, J. L. J. Am. Chem. Soc. 1978, 100, 2584.

12. Stevens, A. E.; Beauchamp, J. L. J. Am. Chem. Soc. 1979, 101, 6449.

13. Heiber, W.; Wagner, G. Z. Naturforschg. 1958, 13b, 339.

14. Using a Born model of solvation: Moelwyn-Hughes, E. A. "Physical Chemistry" 2nd Ed. Pergamon; New York, 1961.

15. Frenz, B. A.; Ibers, J. A. Inorg. Chem. 1972, 11, 1109.

16. Hieber, W.; Hübel, W. Z. Electrochem. 1953, 57, 235.

17. Jolly, P. W.; Pettit, R. J. Am. Chem. Soc. 1966, 88, 5044.

18. Green, M. L. H.; Ishaq, M.; Whiteley, R. N. J. Chem. Soc. A 1967, 1508.

19. Brandt, S.; Helquist, P. J. Am. Chem. Soc. 1979, 101, 6473.

20. Wong, W.-K.; Tam, W.; Gladysz, J. A. J. Am. Chem. Soc. 1979, 101, 5440.

Chapter II

Properties and Reactions of $(CO)_5MnH$ and $(CO)_5MnCH_3$ by Ion Cyclotron Resonance Spectroscopy. A Consideration of Homolytic $D[(CO)_5Mn\text{-}R]$ and Heterolytic $D[(CO)_5Mn^-\text{-}R^+]$ Bond Energies and the Mechanism and Energetics of Reductive Elimination of RH from $(CO)_5Mn(R)H^+$.

Properties and Reactions of $(CO)_5MnH$ and $(CO)_5MnCH_3$ by Ion Cyclotron Resonance Spectroscopy. A Consideration of Homolytic $D[(CO)_5Mn\text{-}R]$ and Heterolytic $D[(CO)_5Mn^-\text{-}R^+]$ Bond Energies and the Mechanism and Energetics of Reductive Elimination of RH from $(CO)_5Mn(R)H^+$

Amy E. Stevens and J. L. Beauchamp

Contribution No. 6327 from the Arthur Amos Noyes Laboratory of Chemical Physics, California Institute of Technology, Pasadena, California 91125, USA

Abstract

The properties and reactions of $(CO)_5MnR$ (R = H, CH_3) are examined using the techniques of ion cyclotron resonance spectroscopy. An examination of the products $(CO)_5Mn(R)H^+$, $(CO)_4Mn(R)H^+$, and $(CO)_5Mn^+$ which result from proton transfer with varying exothermicity to $(CO)_5MnR$ permits several thermochemical and mechanistic inferences. In particular the proton affinities of these species are derived and the mechanism of reductive elimination of RH from the conjugate acids is detailed.

An examination of processes involving negative ions yields the heterolytic bond energies $D[(CO)_5Mn^- - R^+]$. The hydride is found to be an exceptionally strong acid in the gas phase.

An important conclusion of the study is that $D[(CO)_5Mn-CH_3]$ is much stronger than previously thought, being only 5 ± 2 kcal/mol less than $D[(CO)_5Mn-H]$. The electron affinity of the $(CO)_5Mn$ radical is bracketed between the Mn-CH_3 and Mn-H bond energies.

Positive and negative ion mass spectra and ion-molecule reactions are reported briefly.

Introduction

Reductive elimination and its complement, oxidative addition, play major roles in synthetic and catalytic transformations of hydrocarbons effected by transition metal complexes. Only a few studies have been addressed specifically to the kinetics, mechanism, and thermochemistry of these processes.[1-20] Many features of these reactions are puzzling and warrant further investigation. For example, dihydride and bisalkyl complexes tend to be more "stable" than the analogous hydridoalkyl species. Whether this is kinetic or thermodynamic stability is not clear. Several studies indicate reductive elimination does not always occur in a concerted intramolecular step but frequently follows an intermolecular pathway or even one involving hydrocarbon radicals.[6,8,9] Often difficulties arise in determining the reactive intermediate; only indirect evidence can be used to identify the ligands within the coordination sphere of the metal. Finally, there are very few quantitative data that characterize the thermodynamic and activation parameters of these reactions.[16-20]

In this paper we report the gas-phase ion chemistry of $(CO)_5MnCH_3$ and $(CO)_5MnH$, determined by using the techniques of ion cyclotron resonance spectroscopy,[21] which provides some insight into the problems outlined above. This technique provides a nearly collision-free environment, in which highly reactive species are easily formed and characterized. These gas-phase studies allow an assessment of the role of solvent effects on the properties exhibited by these species in solution. Most importantly for this work, the energy

available for a reaction can easily be varied. This energetic control is afforded by protonation studies, using a proton donor BH^+, whose proton affinity (PA) is given by eq. 1. The proton affinities of a wide

$$BH^+ \rightarrow B + H^+ \qquad \Delta H = PA(B) \tag{1}$$

variety of organic bases are known; for example, $PA(NH_3)$ = 207 kcal/mol, and $PA(H_2O)$ = 175 kcal/mol.[22] The usual situation in proton transfer reactions, generalized in eq. 2, is for proton transfer from B_1 to B_2 to occur when $PA(B_2) \geq PA(B_1)$. When the reaction is

$$B_1H^+ + B_2 \rightleftharpoons B_2H^+ + B_1 \tag{2}$$

sufficiently exothermic, excess energy retained by B_2H^+ results in its decomposition. Variation of the donor B_1H^+ can be utilized to quantify the proton affinity of B_2, as well as the energetics of the decomposition of B_2H^+.

In this paper we report protonation reactions of $(CO)_5MnCH_3$ and $(CO)_5MnH$. The negative ion chemistry of these compounds is examined, and the heterolytic bond energies given by eq. 3 determined. Positive

$$(CO)_5MnR \rightarrow (CO)_5Mn^- + R^+ \qquad \Delta H = D[(CO)_5Mn^- - R^+] \tag{3}$$

$$(R = H,\ CH_3)$$

and negative ion mass spectra and the ion-molecule chemistry of these compounds are reported briefly.

Experimental

The techniques of ion cyclotron resonance have been described.[21] The spectrometer used in this study was built in our laboratories and utilizes a 15-in. electromagnet capable of 23.4 kG maximum field. Standard marginal oscillator detection was employed. Pressures were measured with a Schulz-Phelps-type ion gauge calibrated against an MKS Baratron Model 90H1-E capacitance manometer; the estimated uncertainty in absolute pressure, thus in all rate constants, is ± 20%. All electron energies are uncalibrated. All reactions were identified by double resonance techniques;[21] neutrals are not detected.

Pentacarbonylhydridomanganese was prepared by reaction of $Na^+[(CO)_5Mn]^-$ with phosphoric acid.[23] Final purification was effected by pumping on the Dry Ice/acetone-cooled sample until no impurities were observed in the mass spectrum. Pentacarbonylmethylmanganese was prepared by reaction of $Na^+[(CO)_5Mn]^-$ with CH_3I and purified by sublimation;[24] no impurities were detected in the mass spectrum. Decacarbonyldimanganese was obtained from Alfa Inorganics and used as supplied.

All other reagents were used without purification, except for degassing with several freeze-pump-thaw cycles.

Proton transfer reactions were observed under trapped ion conditions, with a typical metal complex:protonation reagent ratio of 1:2 at a total pressure of 5×10^{-7} Torr.

Negative ion mass spectra with zero-energy electrons were taken in the trapping mode, and spectra were recorded following a 3 msec pulse of 70 eV electrons. The electrons were thermalized by using

high pressures of CO_2, as described in the literature.[25] Pressures of the metal complexes were kept low ($1\text{-}4 \times 10^{-8}$ torr) to prevent ion-molecule reactions as well as ensure the electrons were thermalized before attachment.

All auxiliary thermochemical data are given in Table I.

Table I. Additional Thermochemistry Used in This Work[a]

Species	ΔH_f°	Reference
CH_4	-17.89	b
CH_3	34.82	b
H	52.09	b
H^+	365.7	c
H^-	33.39	c
$IP[(CO)_5MnH]$	8.55 ± 0.1 eV	d
$IP[(CO)_5MnCH_3]$	8.3 ± 0.1 eV	e

a. All values in kcal/mol at 298 K except as noted.

b. Stull, D. R.; Prophet, H. Natl. Stand. Ref. Data Ser., Natl. Bur. Stand. 1971, No. 37.

c. Wagner, D. D.; Evans, W. H.; Parker, V. B.; Halow, I.; Bailey, S. M.; Schumm, R. J.; Natl. Bur. Stand. Tech. Note 270-3, 1968.

d. Hall, M. B. J. Am. Chem. Soc. 1975, 97, 2057.

e. Lichtenberger, D. L.; Fenske, R. F. Inorg. Chem. 1974, 13, 486.

Results

Mass Spectra of $(CO)_5MnH$ and $(CO)_5MnCH_3$. The positive ion mass spectra of $(CO)_5MnH$ and $(CO)_5MnCH_3$ recorded on our instrument agree well with those reported in the literature.[26,27] The 70 eV negative ion mass spectrum of $(CO)_5MnH$, taken in the drift mode at a pressure of 3×10^{-7} Torr, yields the ions $(CO)_5Mn^-$ (6%), $(CO)_4MnH^-$ (91%), and $(CO)_3MnH^-$ (3%). The spectrum is unchanged from 70 eV to 0.5 eV. The negative ion spectrum with zero-energy electrons (1:90 to 1:400 mixture of $(CO)_5MnH$ with CO_2) shows 100% $(CO)_4MnH^-$.

The 70 eV negative ion mass spectrum of $(CO)_5MnCH_3$, taken in the drift mode at a pressure of 1.5×10^{-7} Torr, yields the ions $(CO)_5Mn^-$ (10%), $(CO)_4MnCH_3^-$ (82%) and $(CO)_3MnCH_3^-$ (8%). This does not change with electron energy except near 0 eV, where the ion abundance is roughly $(CO)_5Mn^-$ (5%), $(CO)_4MnCH_3^-$ (57%) and $(CO)_3MnCH_3^-$ (38%). The negative ion spectrum with zero-energy electrons (1:700 to 1:1340 mixture of $(CO)_5MnCH_3$ with CO_2) yields the ions $(CO)_5Mn^-$ (86%) and $(CO)_4MnCH_3^-$ (14%). The ratio of these ions does not vary over the range of CO_2 pressures investigated, nor over trapping times of 0-80 msec.

Ion-molecule chemistry in $(CO)_5MnH$. The positive ion-molecule chemistry of $(CO)_5MnH$ at 1.5×10^{-6} Torr is dominated by rapid, extensive clustering of all the ions, except parent, produced by 70 eV ionization. An example is afforded by the reaction of MnH^+, eq. 4.

$$MnH^+ + (CO)_5MnH \rightarrow (CO)_4Mn_2^+ + CO + H_2 \qquad (4)$$

Within 30 msec following a 10 msec electron pulse, the total intensities

of ions from m/e 200-395 are comparable to those of lower mass. Since our spectrometer does not have the unit mass resolution necessary to differentiate the various product ions, no attempt was made to quantify these reactions, or to observe ions with mass greater than 395.

Besides the clustering reactions, Mn^+ undergoes charge-transfer to produce $(CO)_nMnH^+$, n = 1-5, and $(CO)_5Mn^+$. The latter product may be due to H^- transfer. Since IP[Mn] = 7.432 eV (Table II) is less than IP$[(CO)_5MnH]$ = 8.55 eV (Table I), this indicates substantial amounts of excited Mn^+ are produced. Table II lists several of the low-lying excited states of Mn^+; these are undoubtedly easily accessible with 70 eV electron impact ionization.

Finally, $(CO)_5MnH_2^+$ is observed from reaction 5. Figure 1

$$(CO)_5MnH^+ + (CO)_5MnH \rightarrow (CO)_5MnH_2^+ + (CO)_5Mn \qquad (5)$$

illustrates the temporal variation of the ions $(CO)_5MnH^+$ and $(CO)_5MnH_2^+$ following a 9 eV electron beam pulse; a rate constant of 1.8×10^{-10} cm^3-$molec^{-1}$-s^{-1} for reaction 5 is derived from these data. The ion product of reaction 5 is unreactive with $(CO)_5MnH$.

The negative ion-molecule chemistry of $(CO)_5MnH$ at 4×10^{-10} Torr shows no products which can be attributed to reactions with the hydride. At longer times, small amounts of $Mn_2(CO)_9^-$ and $Mn_2(CO)_8^-$ arise from $(CO)_4MnH^-$, and $Mn_2(CO)_7^-$ from $(CO)_3MnH^-$. These ions are attributed to charge transfer with $Mn_2(CO)_{10}$, present in trace amounts from decomposition of $(CO)_5MnH$; addition of $Mn_2(CO)_{10}$ increases the abundance of these ions dramatically.

Table II. Low-Lying Excited States of Mn^{+}[a]

State	Level
a^7S	0.00 IP(Mn) = 7.432 eV
a^5S	1.17
a^5D	1.78
a^5G	3.42
a^3P	3.70
a^5P	3.71
a^3H	3.78
a^3F	3.91

a. Moore, C. E. "Atomic Energy Levels, Vol. 2," National Bureau Standards: Washington, 1971. All values in eV; only the level for the lowest-lying J is given.

FIGURE 1. Temporal variation of the abundances of $(CO)_5MnH^+$ and $(CO)_5MnH_2^+$, observed in 1.6×10^{-7} Torr $(CO)_5MnH$, following a 10 msec, 9 eV electron pulse.

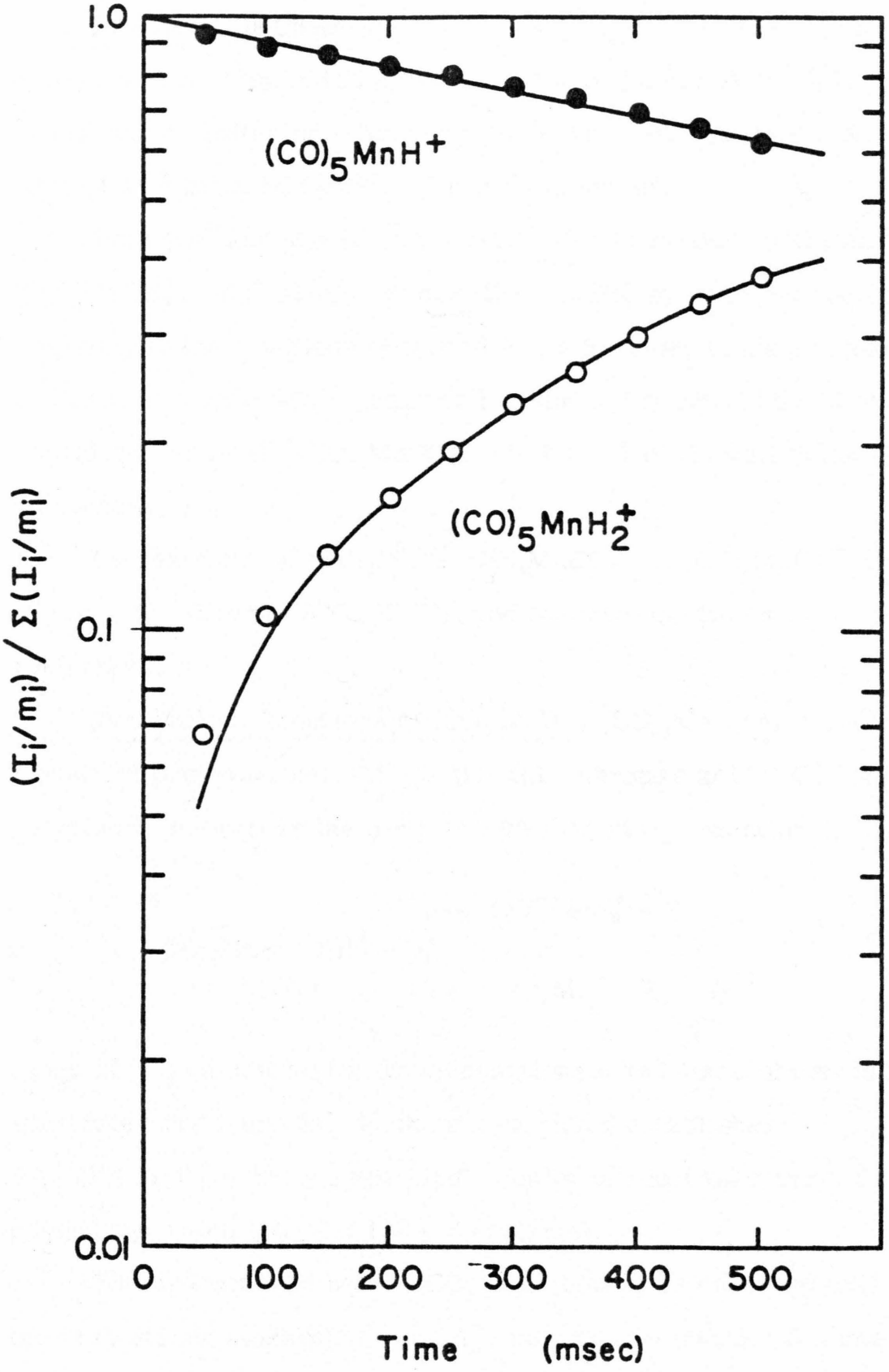
1.0
0.1
0.01
$(CO)_5MnH^+$
$(CO)_5MnH_2^+$
$(I_i/m_i) / \Sigma(I_i/m_i)$
0
100
200
300
400
500
Time (msec)

Ion-Molecule Chemistry in $(CO)_5MnCH_3$. The positive ion-molecule chemistry of $(CO)_5MnCH_3$ at 4×10^{-7} Torr is characterized by extensive clustering. Ions up to m/e 395 were observed, but no attempt was made to further quantify this sytem.

Both Mn^+ and $MnCH_3^+$ charge-transfer to produce $(CO)_5Mn^+$ and $(CO)_5MnCH_3^+$. Mn^+ also produces $(CO)_4MnCH_3^+$ by charge-transfer. Similarly to the reactions observed in the hydride, these are taken as evidence of excited Mn^+ (and possibly $MnCH_3^+$) produced by 70 eV ionization, since IP $[(CO)_5MnCH_3] = 8.3 \pm 0.1$ eV is well below that of manganese.

No reactions of $(CO)_5Mn^-$, $(CO)_4MnCH_3^-$, of $(CO)_3MnCH_3^-$ are seen at 1.4×10^{-7} Torr of $(CO)_5MnCH_3$ and ion trapping times as long as 1000 msec.

Protonation Reactions of $(CO)_5MnH$. $(CO)_5MnH$ reacts with a variety of proton donors BH^+ to give the conjugate acid $(CO)_5MnH_2^+$, reaction 6, as well as the product with loss of H_2, reaction 7. The

$$(CO)_5MnH + BH^+ \longrightarrow \begin{cases} (CO)_5MnH_2^+ + B & (6) \\ (CO)_5Mn^+ + H_2 + B & (7) \end{cases}$$

range of proton donors for which reactions 6 and 7 are observed is illustrated in Figure 2a. Onset of reaction 6 establishes PA $[(CO)_5MnH] = 204 \pm 3$ kcal/mol. Onset of reaction 7 occurs with donors for which PA(B) $\leq 198 \pm 3$ kcal/mol.

The product with loss of CO, $(CO)_4MnH_2^+$, is observed only with the very strong acids HCO^+ or CH_5^+, as given in reaction 8. Inter-

FIGURE 2. a) Range of proton donors for which the products $(CO)_5MnH_2^+$ (reaction 6) and $(CO)_5Mn^+$ (reaction 7) are observed from protonation reactions of $(CO)_5MnH$.

b) Range of proton donors for which the products $(CO)_5Mn^+$ (reaction 9), $(CO)_5Mn(CH_3)H^+$ (reaction 10), and $(CO)_4Mn(CH_3)H^+$ (reaction 11) are observed from protonation reactions of $(CO)_5MnCH_3$. The proton affinity (kcal/mol) of each base examined, $PA(B)-PA(NH_3)$, is given in parentheses.

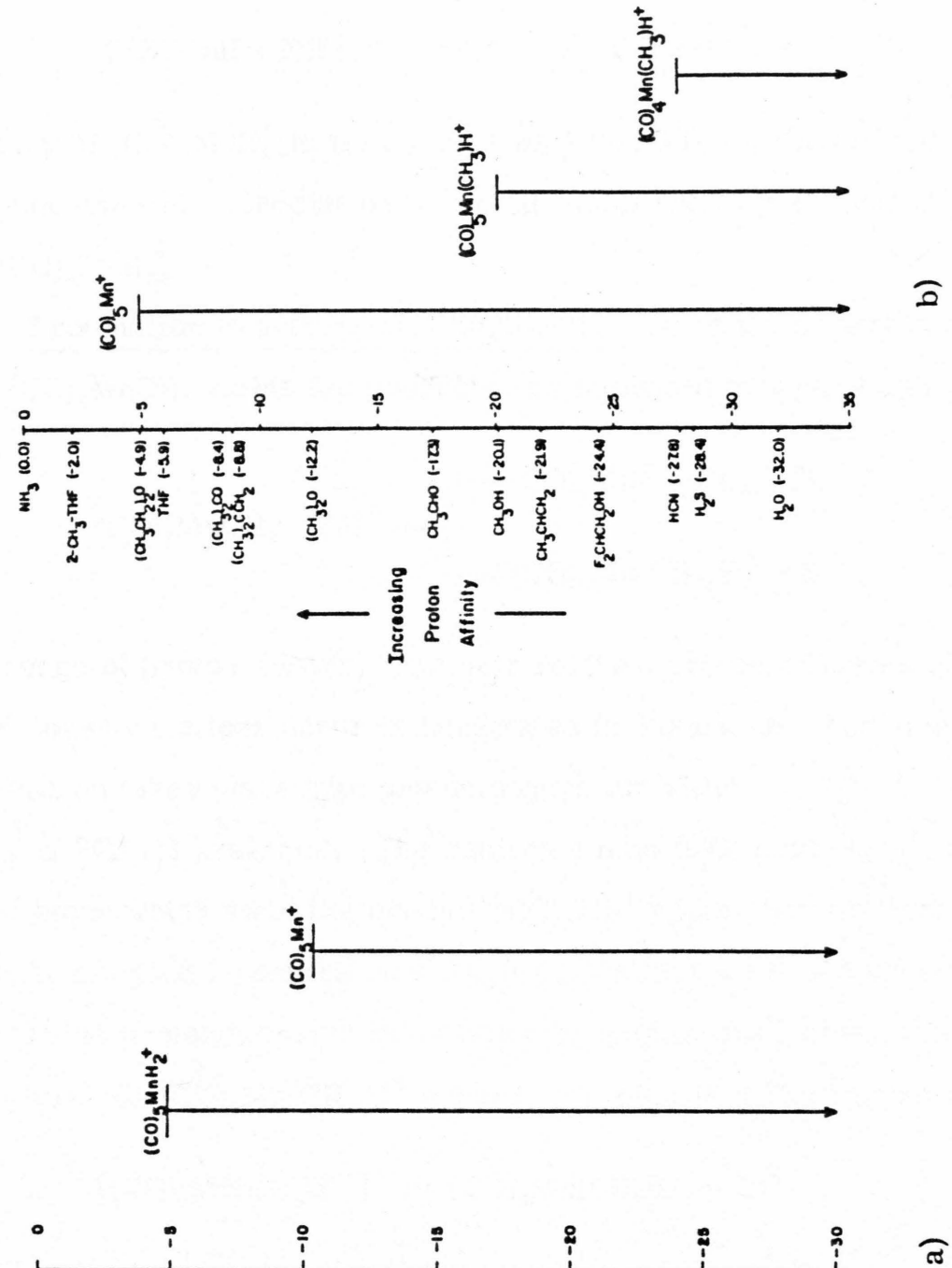
Increasing Proton Affinity
NH3 (0.0)
2-CH3-THF (-2.0)
(CH3CH2)2O (-4.9)
THF (-5.9)
(CH3)2CO (-8.4)
(CH3)2CHCN (-10.1)
CH3CH2CH2CH2CN (-10.4)
(CH3)2O (-12.2)
CH3CH2CHO (-14.3)
CH3CN (-15.3)
HCN (-27.8)
(CO)5MnH2+
(CO)5Mn+
(CO)5Mn(CH3)H+
(CO)4Mn(CH3)H+
(CH3)3O (-12.2)
CH3CHO (-13.2)
CH3OH (-20.1)
CH3CHCH2 (-21.9)
F2CHCH2OH (-24.4)
H2S (-28.4)
H2O (-32.0)
a)
b)

$$(CO)_5MnH + BH^+ \rightarrow (CO)_4MnH_2^+ + CO + B \qquad (8)$$

mediacy of $(CO)_5MnH_2^+$ in both reactions 7 and 8 is established by collision-induced dissociation of the dihydride ion to yield both $(CO)_5Mn^+$ and $(CO)_4MnH_2^+$.

Protonation Reactions of $(CO)_5MnCH_3$. Reaction of proton donors with $(CO)_5MnCH_3$ yields the products as indicated by eqs. 9 and 10.

$$(CO)_5MnCH_3 + BH^+ \begin{cases} \rightarrow (CO)_5Mn^+ + CH_4 + B & (9) \\ \rightarrow (CO)_5Mn(CH_3)H^+ + B & (10) \end{cases}$$

The range of proton donors, and their relative proton affinities, for which these reactions occur is illustrated in Figure 2b. Methane elimination takes place with proton donors for which $PA(B) \leq 203 \pm 3$ kcal/mol. The conjugate acid $(CO)_5Mn(CH_3)H^+$ is below those which yield the product $(CO)_5Mn^+$ as an abundant ion; onset of reaction 10 establishes $PA[(CO)_5MnCH_3] = 188 \pm 3$ kcal/mol.

If the proton transfer is sufficiently exothermic, dissociation of the product $(CO)_5Mn(CH_3)H^+$ occurs, reaction 11. Decomposition

$$[(CO)_5Mn(CH_3)H^+]^* \rightarrow (CO)_4Mn(CH_3)H^+ + CO \qquad (11)$$

with loss of CO is observed with donors less basic than HCN, indicating $D[(CO)_4Mn(CH_3)H^+\text{-}CO] \cong 7 \pm 2$ kcal/mol. Intermediacy of $(CO)_5Mn(CH_3)H^+$ in reaction 11 is evidenced by collision-induced dissociation of this ion to yield $(CO)_4Mn(CH_3)H^+$. Loss of CH_4 cannot be collisionally induced.

The products $(CO)_5Mn^+$, $(CO)_4MnH_2^+$, and $(CO)_4Mn(CH_3)H^+$ undergo

rapid exchange of the CO ligands with all of the compounds B used in the protonation reactions, as well as loss through clustering reactions. These further reactions precluded the possibility of measuring quantitative product distributions or proton transfer rates for reactions 6-11.

Metal Hydrogen Homolytic Bond Energies. The homolytic bond dissociation energy in a protonated compound, $D(B^+-H)$, can be calculated from the proton affinity and adiabatic ionization potential, as given in eq. 12. Using the values for the adiabatic ionization potentials

$$D(B^+-H) = PA(B) + IP(B) - IP(H) \qquad (12)$$

of $(CO)_5MnH$ and $(CO)_5MnCH_3$ given in Table I with the proton affinities determined for this work yield the homolytic manganese-hydrogen bond energies, $D[(CO)_5MnH^+-H] = 87 \pm 3$ kcal/mol, and $D[(CO)_5MnCH_3^+-H] = 67 \pm 3$ kcal/mol.

Reaction of Trimethyl Silyl Ion with $(CO)_5MnH$. $(CH_3)_3Si^+$ reacts with $(CO)_5MnH$ in a 6:1 mixture of $(CH_3)_4Si$ with $(CO)_5MnH$ at a total pressure of 7×10^{-7} Torr according to reactions 13-15. Product ratios

$$(CH_3)_3Si^+ + (CO)_5MnH \xrightarrow{66\%} (CO)_4Mn(H)Si(CH_3)_3^+ + CO \qquad (13)$$

$$(CH_3)_3Si^+ + (CO)_5MnH \xrightarrow{11\%} (CO)_3Mn(H)Si(CH_3)_3^+ + 2CO \qquad (14)$$

$$(CH_3)_3Si^+ + (CO)_5MnH \xrightarrow{23\%} (CO)_5Mn^+ + HSi(CH_3)_3 \qquad (15)$$

are only approximate, as $(CO)_5Mn^+$ is lost through clustering with $(CO)_5MnH$. The intensity of $(CO)_3Mn(H)Si(CH_3)_3^+$ reached a maximum at 200 msec (total trapping time 500 msec); it is uncertain whether only vibrationally excited $(CH_3)_3Si^+$ produced this ion or whether it is lost

to clustering reactions as well.

The hydride transfer reaction 15 provides a limit for the heterolytic bond energy, $D[(CO)_5Mn^+-H^-] \leq D[(CH_3)_3Si^+-H^-] = 220.1 \pm 0.7$ kcal/mol.[28]

Proton Affinity and Methyl Cation Affinity of $(CO)_5Mn^-$. The negative ions $X^- = F^-$, Cl^- and $CF_3CO_2^-$ all react with $(CO)_5MnH$ according to eq. 16. The reverse of reaction 16 is not observed in a

$$(CO)_5MnH + X^- \rightarrow (CO)_5Mn^- + XH \qquad (16)$$

10:1 mixture of CF_3CO_2H with $(CO)_5MnH$ at a total pressure of 4.4×10^{-7} Torr. After 500 msec the 1.3:1 ion intensity ratio of $(CO)_5Mn^-$ to $CF_3CO_2^-$ indicates $D[(CO)_5Mn^-H^+] \leq D[CF_3CO_2^-H^+] - 1.8$ kcal/mol.

For $X^- = I^-$ reaction 16 did not occur. Rather, the reverse reaction, in which $(CO)_5Mn^-$ (produced from $Mn_2(CO)_{10}$) abstracts a proton from HI to give I^- is observed, indicating $D[(CO)_5Mn^-H^+] \geq D[I^-H^+]$. Equilibrium could not be established in a mixture of $(CO)_5MnH$ and HI, since the $(CO)_5Mn^-$ reacted rapidly with a trace of chlorine-containing neutral contaminant.

The proton affinity of $(CO)_5Mn^-$ is bracketed between 314.3 and 320.9 kcal/mol; $D[(CO)_5Mn^-H^+] = 318 \pm 3$ kcal/mol is assumed.[29] The absence of additional reference species with an acidity within this range precluded further refinement of this value.

The negative ions $X^- = F^-$ and Cl^- react with $(CO)_5MnCH_3$, reaction 17. For $X^- = I^-$ the reverse reaction is observed. For $X^- = Br^-$ the reaction is not observed to proceed in either the forward

$$(CO)_5MnCH_3 + X^- \rightarrow (CO)_5Mn^- + CH_3X \qquad (17)$$

or reverse direction; apparently it is much too slow to be observed for this particular combination of nucleophiles on the ICR time scale. The methyl cation affinity is thus bound between that of I^- and Cl^-, 211.8 and 224.5 kcal/mol, respectively.[30] A value for $D[(CO)_5Mn^- - CH_3^+]$ = 218 ± 6 kcal/mol is assumed.

Discussion

Mass Spectra and Ion Molecule Chemistry. The most prevalent feature of the positive ion-molecule reactions of organometallics such as $(CO)_5Fe$,[31] $(CO)_4Ni$,[32] $(\eta^5\text{-}C_5H_5)_2Fe$,[33] $(\eta^5\text{-}C_5H_5)_2Ni$,[34] and $(\eta^5\text{-}C_5H_5)Ni(NO)$[28] is the rapid clustering to form multi-nuclear metal ions; this is the case for $(CO)_5MnH$ and $(CO)_5MnCH_3$ as well. The evidence for formation of electronically excited Mn^+ by electron impact ionization is not unique to these molecules; Fe^+ formed from $(CO)_5Fe$ undergoes charge-transfer with $(CO)_5Fe$, indicative of excited state formation.

The negative ion mass spectra of these complexes are similar to those of other metal carbonyls;[35] no molecular ion is observed, the predominant fragmentation occurs by loss of CO, and to a much lesser extent loss of the σ-bonding ligand occurs. The ion-molecule chemistry of these compounds is unusual in that no clustering of the negative ions is observed.

$(CO)_5Mn^-$ is not produced from $(CO)_5MnH$ by capture of zero-energy electrons; this indicates the electron affinity $EA[(CO)_5Mn] \leq D[(CO)_5Mn\text{-}H]$. By contrast, $(CO)_5Mn^-$ is produced from $(CO)_5MnCH_3$, which establishes $EA[(CO)_5Mn] \geq D[(CO)_5Mn\text{-}CH_3]$. These provide limits for the heterolytic bond energies, $D[(CO)_5Mn^-\text{-}H^+] \geq 318.6$ kcal/mol, and $D[(CO)_5Mn^-\text{-}CH_3^+] \leq 226.9$ kcal/mol; these data are consistent with the values $D[(CO)_5Mn^-\text{-}H^+ = 318 \pm 3$ kcal/mol and $D[(CO)_5Mn^-\text{-}CH_3^+] = 218 \pm 6$ kcal/mol determined by reaction of nucleophiles with these compounds.

Proton Transfer Reactions. Reaction of $(CO)_5MnH$ with proton donors follows the pattern of reactivity outlined in the introduction. The conjugate acid $(CO)_5MnH_2^+$ is produced from proton donors for which PA(B) $\leq$ 204 kcal/mol. On increasing the exothermicity of the proton transfer, with donors for which PA(B) $\leq$ 198 kcal/mol, the elimination of H_2 takes place. Intermediacy of $(CO)_5MnH_2^+$ in the reaction with H_2 loss, reaction 7, is evidenced by the collision-induced dissociation of this ion to yield $(CO)_5Mn^+$. We assume that the H_2 elimination does not take place with donors for which PA(B) $\geq$ 198 kcal/mol because it is endothermic.

The difference in proton affinity values for the onsets of reactions 6 and 7 establishes the binding energy $D[(CO)_5Mn^+-H_2] = 6 \pm 2$ kcal/mol. This value can be taken with D[H-H] to give an average value of 55 kcal/mol for the two metal-hydrogen bond energies. It is noted however, that the first bond energy, $D[(CO)_5MnH^+-H]$ is 87 $\pm$ 3 kcal/mol, while the second is calculated from eq. 18 to be $D[(CO)_5Mn^+-H] = 23 \pm 3$ kcal/mol.

$$D[(CO)_5Mn^+-H] = IP[H] - IP[(CO)_5MnH] + D[H-H] - (198 \pm 3 \text{ kcal/mol}) \quad (18)$$

These thermochemical data are unusual in several respects. First, the proton affinity of the hydride is 15 kcal/mol greater than that of $(CO)_5MnCH_3$. This is in direct contrast to all organic bases, for which methyl substitution at the protonated center increases the proton affinity, typically by 10-15 kcal/mol.[22] Second, the bond energy $D[(CO)_5MnH^+-H] = 87$ kcal/mol, is 20 kcal/mol stronger than

$D[(CO)_5MnCH_3^+-H]$, and is the strongest metal-hydrogen bond yet measured for a metal complex.[16,18,36-38] Third, either H_2 or CO may be lost on collisional excitation of $(CO)_5MnH_2^+$.

These data suggest there is a strong H-H interaction in $(CO)_5MnH_2^+$; it might best be visualized as H_2 coordinated to $(CO)_5Mn^+$, with the site of protonation the manganese-hydrogen bond, I, as illustrated in Figure 3. The 6 kcal/mol binding energy of H_2 is comparable to $D[Li^+-H_2]$ = 5-6 kcal/mol derived from ab initio SCF calculations,[39] and $D[CH_3CH_2^+-H_2]$ = 4 kcal/mol and $D[H_3^+-H_2]$ = 9.6 kcal/mol derived from high-pressure mass spectrometry.[40] In each of these examples the H-H bond has not been broken. It is also in reasonable agreement with $D[IrCl(PPh_3)_3-H_2]$ = 14 kcal/mol,[16] the estimated $D[(\eta^5-C_5H_5)_2Mo-H_2] \cong 16$ kcal/mol and $D[(\eta^5-C_5H_5)_2W-H_2] \cong 42$ kcal/mol,[19] and $D[(PH_3)_2Pt-H_2] \cong 5$ kcal/mol.[41] In these examples the H_2 bond has been broken to form two sigma bonds to the metal.

A reaction coordinate for $(CO)_5Mn^+/H_2$ is illustrated in Figure 4a, in which no information about the activation barrier for unimolecular H_2 loss can be obtained from these data; the above interpretation requires no activation energy in excess of the endothermicity of H_2 loss. The data are, however, consistent with protonation on the metal center, site II illustrated in Figure 3, with a strong H-H interaction and an activation barrier for H_2 loss low enough to be competitive with CO loss.

The protonation reactions of $(CO)_5MnCH_3$ are particularly surprising in that the conjugate acid $(CO)_5Mn(CH_3)H^+$ is produced only from proton donors whose proton affinity is substantially below those

FIGURE 3. Species resulting from protonation on the Mn-R bond, site I, and protonation on the metal center, site II, of $(CO)_5MnR$.

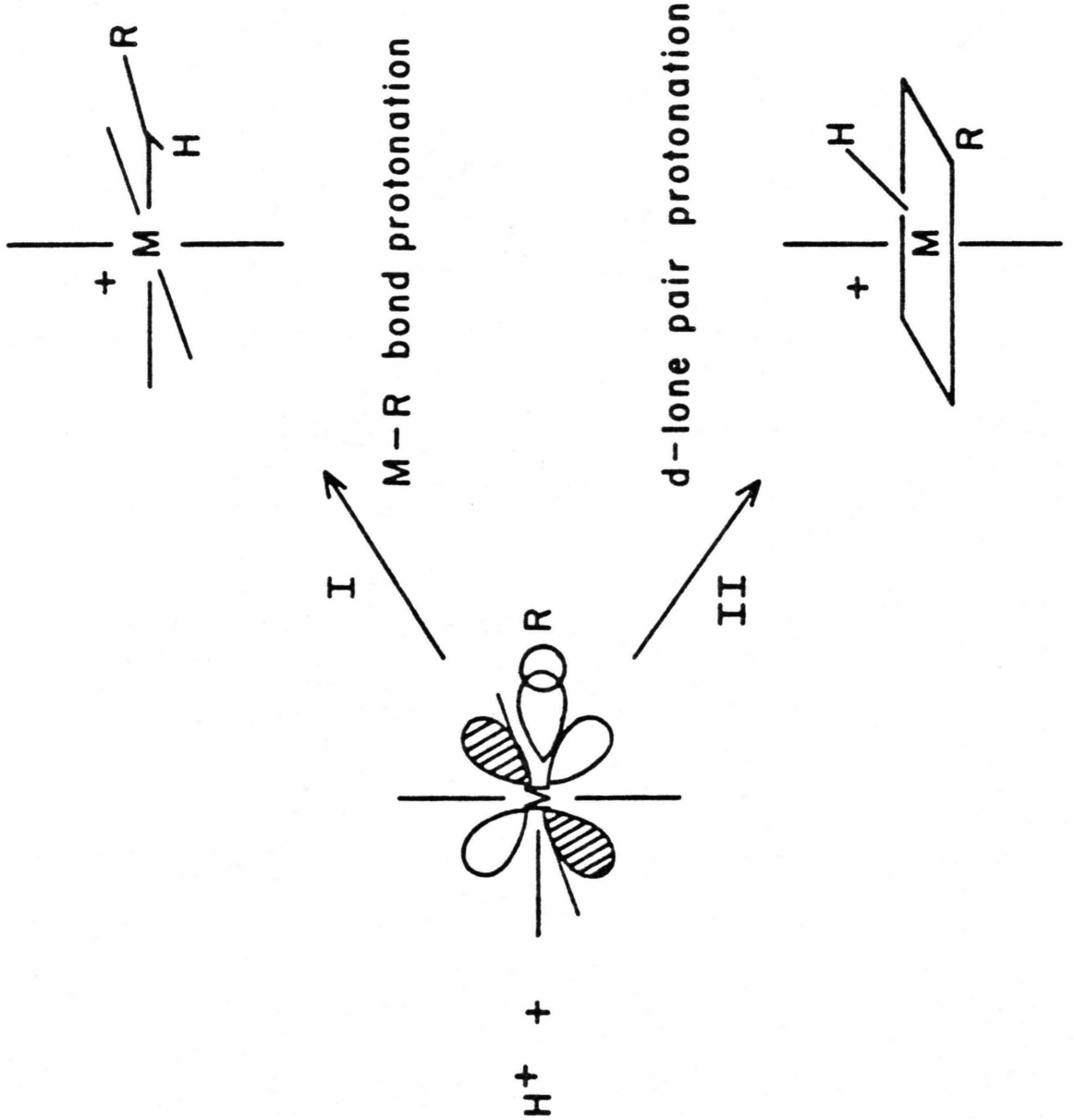
R
H
M
+
M–R bond protonation
d–lone pair protonation
I
II
R
H
M
+
H+ +

FIGURE 4. a) Energetic relationships between species resulting from reductive elimination of H_2 from protonated $(CO)_5MnH$.

b) Energetic relationships between species resulting from reductive elimination of CH_4 or CO from protonated $(CO)_5MnCH_3$.

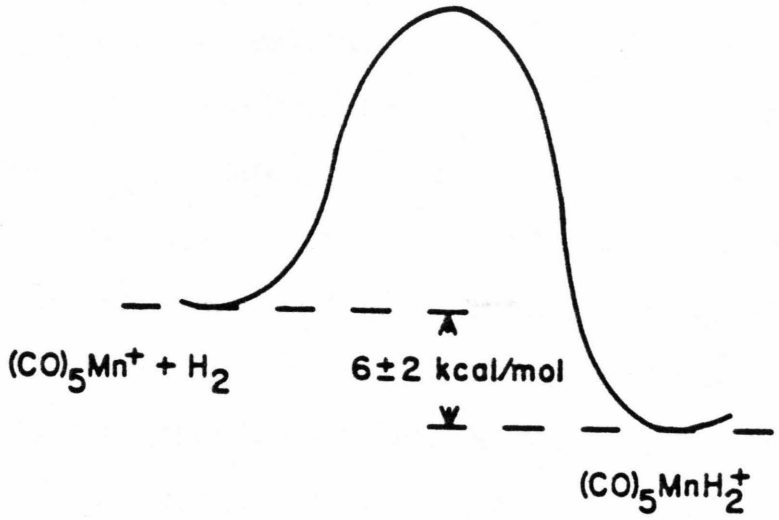
$(CO)_5Mn^+ + H_2$
6±2 kcal/mol
$(CO)_5MnH_2^+$

a)

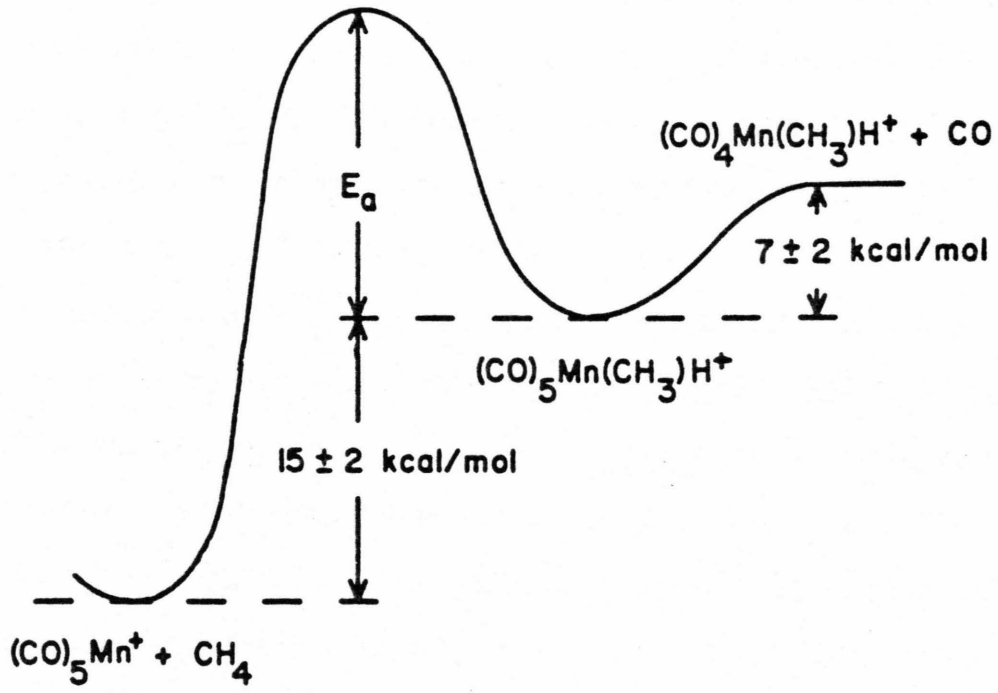
$(CO)_4Mn(CH_3)H^+ + CO$
E_a
7 ± 2 kcal/mol
$(CO)_5Mn(CH_3)H^+$
15 ± 2 kcal/mol
$(CO)_5Mn^+ + CH_4$

b)

which yield $(CO)_5Mn^+$ as an abundant ion. We interpret this as evidence for two available reactive sites on $(CO)_5MnCH_3$; reactions 9 and 10 are not competitive in the sense of having common or readily interconverted intermediates. We propose that protonation of the manganese-methyl bond leads to formation of methane with little or no activation barrier; for PA(B) > 203 kcal/mol, methane loss (reaction 9) is not observed because it is endothermic. Protonation on the metal center forms a kinetically stable protonated complex. Since this species has not been observed in solution, we have only indirect evidence $(CO)_5Mn(CH_3)H^+$ is a hydridomethyl species. This includes: first, protonation of methyl or hydrido complexes in solution results in hydridomethyl or dihydrido ions of cis conformation.[4,42] Second, the manganese hydride bond dissociation energy of 67 ± 3 kcal/mol is comparable to those of other first-row transition metal hydrides.[36] Third, $(CO)_5Mn(CH_3)H^+$ does not react further with bases present, an indication of full (18-electron) coordination at the manganese. This indicates the 15 ± 2 kcal/mol difference in proton affinity values for the onsets of reactions 9 and 10 is the endothermicity of oxidative addition of CH_4 to $(CO)_5Mn^+$.

Decomposition according to reaction 11, in which CO is lost in preference to CH_4, indicates $D[(CO)_4Mn(CH_3)H^+\text{-}CO] \cong 7$ kcal/mol. Again, this value depends only on the difference in the proton affinity values for the onsets of reaction 10 and 11. The loss of CH_4 is not competitive with CO loss in collision-induced dissociation. Unimolecular reductive elimination of methane from $(CO)_5Mn(CH_3)H^+$ must therefore have an activation energy for CH_4 elimination in excess

of 7 kcal/mol. These results are summarized in Figure 4b, in which the activation energy E_a for elimination of methane cannot be determined from these experiments.

Comparison to Solution Studies. $(CO)_5MnCH_3$ in solution reacts with acids with elimination of methane;[15,42] a reaction mechanism involving oxidative addition of undissociated acid followed by reductive elimination of methane has been suggested.[15] $(CO)_5MnH$ reacts with neat HO_3SCF_3 to yield H_2 and $[Mn(CO)_5^+][O_3SCF_3^-]$; no mechanism is proposed for this reaction.[43] These observations are in agreement with the thermodynamic instability of $(CO)_5Mn(CH_3)H^+$ predicted from these studies. The 6 kcal/mol binding of H_2 to $(CO)_5Mn^+$ observed in the gas phase could easily be countered by an ion-pair association of $[O_3SCF_3^-]$ with $[(CO)_5Mn^+]$ in solution.

Examples of the difference in stability between the isoelectronic dihydrides and hydridomethyl complexes can be found.[2-4,10] Protonation of $[P(OCH_3)_3]_4CoCH_3$ in methanol or acetone leads to rapid (ca. 31% complete in 10 min at -70°) methane evolution; the presumed intermediate, $[P(OCH_3)_3]_4Co(CH_3)H^+$, is not detectable.[4] Protonation of $[P(OCH_3)_3]_4CoH$, by contrast, yields $[P(OCH_3)_3]_4CoH_2^+$, which is isolable as the PF_6^- salt, and decomposes with a 13.2 hour half-life at room temperature.[4] The compounds $(\eta^5\text{-}C_5H_5)_2W(CH_3)H$, $(CO)_4Os(CH_3)H$, and $(\eta^5\text{-}C_5Me_5)_2Zr(CH_2CHMe_2)H$ are also less thermally stable than the analogous dihydrides.[2,3,10]

Comparison to Gas-Phase Protonation Studies. The existence of two protonation sites is not unique to $(CO)_5MnCH_3$. Stronger acids will protonate ketene in the gas phase to form CH_2COH^+ as well as the more

stable CH_3CO^+; no information is available on a barrier to isomerization.[44] More unusual effects are reported in the protonation of allene and propyne, for which reaction with mild protonating agents (H_3O^+, $C_3H_4^+$) results in $C_3H_5^+$ of predominantly the 2-propenyl structure, rather than the more stable allyl cation. Increasing the exothermicity of the proton transfer (CH_5^+, $C_2H_5^+$ as protonating agents) increases the percentage of the allyl isomer. This is interpreted as evidence for a barrier not only to interconversion of the allyl and 2-propenyl isomers, but also to protonation at the central carbon of allene.[45] Another example of proton transfer occurring from donors whose proton affinity is greater than that of the acceptor, as occurs for $(CO)_5MnCH_3$, is afforded by protonation reactions of trans-2-butene and cyclohexene. Trans-2-butene will react with proton donors whose proton affinity exceeds that of trans-2-butene to form the t-butyl ion. Cyclohexene also undergoes a protonation-isomerization reaction to yield exclusively the methylcyclopentyl ion.[46]

Electronic Structure of $(CO)_5Mn^+$. The large difference between $D[(CO)_5Mn^+-H]$ = 23 kcal/mol and $D[(CO)_5MnH^+-H]$ = 87 kcal/mol suggests that $(CO)_5Mn^+$ has a singlet ground state. Forming the first bond to hydrogen requires a substantial electronic, and possibly geometrical, rearrangement, whereas the radical $(CO)_5MnH^+$ readily forms a strong σ-bond. Several molecular orbital calculations predict the d^6 pentacarbonyls to have singlet states with square pyramidal (C_{4v}) geometry.[47] The infra-red and electronic spectra of $[(CO)_5Mn^+][O_3SCF_3^-]$ in HO_3SCF_3 are also consistent with this interpretation.[43]

The oxidative addition of methane can also be broken into two steps, eqs. 19 and 20, in which the first bond, whether H or CH_3, is much weaker than the second.

$$(CO)_5Mn^+ + CH_3 + H \xrightarrow{22\ kcal/mol} (CO)_5MnCH_3^+ + H \xrightarrow{67\ kcal/mol} (CO)_5Mn(CH_3)H^+ \quad (19)$$

$$(CO)_5Mn^+ + CH_3 + H \xrightarrow{23\ kcal/mol} (CO)_5MnH^+ + CH_3 \xrightarrow{66\ kcal/mol} (CO)_5Mn(CH_3)H^+ \quad (20)$$

Hydride Affinity of $(CO)_5Mn^+$. The heterolytic bond energy, $D[(CO)_5Mn^+ - H^-] = 202 \pm 3$ kcal/mol is calculated from the onset of H_2 loss, reaction 7, by eq. 21. This is the lowest hydride affinity ever

$$D[(CO)_5Mn^+ - H^-] = IP(H) + D(H - H) - EA(H) - (198 \pm 3\ kcal/mol) \quad (21)$$

measured; all carbon and silicon ions studied have substantially greater hydride affinities.[28] This value is supported by the hydride transfer from $(CO)_5MnH$ to $(CH_3)_3Si^+$, reaction 15, which demonstrates $D[(CO)_5Mn^+ - H^-] \leq 220.1 \pm 0.7$ kcal/mol.

Gas Phase Acidity of $(CO)_5MnH$. $(CO)_5MnH$ is an extremely strong acid in the gas phase, with $D[(CO)_5Mn^- - H^+] = 318 \pm 3$ kcal/mol, making its acidity comparable to that of HI and HBr. By contrast, $(CO)_5MnH$ in aqueous solution is only weakly acidic, with a $pk_a = 7.1$.[48] This difference is due to the very poor solvation of $(CO)_5Mn^-$.

The strong gas-phase acidity results from a weak manganese-hydrogen bond and a high electron affinity (EA) of the $(CO)_5Mn$ radical, as given in eq. 22. The bond energy $D[(CO)_5Mn\text{-}H]$ has been determined

$$D[(CO)_5Mn^- - H^+] = D[(CO)_5Mn\text{-}H] - EA[(CO)_5Mn] + IP(H) \qquad (22)$$

in the gas phase by thermochemical data to be 57 kcal/mol.[37] A kinetic determination in benzene solution has yielded a higher value, 64 ± 1 kcal/mol.[38] Using the value $D[(CO)_5Mn\text{-}H] = 57$ kcal/mol in eq. 22 yields $EA[(CO)_5Mn] = 2.3 \pm 0.2$ eV.

Ion cyclotron resonance studies of $(CO)_5Mn^-$ have indicated no "photodisappearance" of the ion when irradiated by photons in the range 1.55 to 4.1 eV.[49] This was interpreted as a lack of an optical absorption of $(CO)_5Mn^-$ within this range, since a number of metal carbonyl anions photodissociate by CO loss when irradiated. The calculation of a 2.3 eV electron affinity indicates also that the cross-section for electron detachment must be extremely small at these energies; the vertical electron affinity is substantially greater than the adiabatic electron affinity. This is not surprising when the structures of the anion and radical are considered. The crystal structure of $[Ni(1,10\text{-phenanthroline})_3][Mn(CO)_5]_2$ shows $(CO)_5Mn^-$ to be trigonal bipyramidal (D_{3h}),[50] while analysis of the C-O stretching modes of $(CO)_5Mn$ isolated in an Ar matrix has indicated it takes on a square pyramidal (C_{4v}) geometry.[51] Changes in the Mn-C and C-O bond distances are also expected. A large difference between the adiabatic and vertical electron affinity is evident for SF_6, with an adiabatic electron affinity of 0.6 eV,[52] but a vertical electron affinity approximately 3.1 eV.[53] This large difference arises from an increase of about 0.1 Å in the S-F bond distances on forming the anion. Another example is afforded by $(CO)_4Fe^-$, which gives a very broad photo-

electron spectrum and only a very weak signal. This ion, for which the relaxation energy is expected to be more comparable to that of $(CO)_5Mn^-$, showed competition from CO loss at the irradiating energy; no vertical EA was reported, and the adiabatic EA is difficult to assign.[54]

Methyl Cation Affinity of $(CO)_5Mn^-$. The determination of $D[(CO)_5Mn^- - CH_3^+] = 218 \pm 6$ kcal/mol is somewhat disappointing in that no reaction could be identified in mixtures of CH_3Br with $(CO)_5MnCH_3$, causing the rather large error limits. The slowness of the reaction is not unexpected; not only is Br^- a poor nucleophile,[55] but $(CO)_5Mn^-$, with a low methyl cation affinity, substantial charge delocalization, and high polarizability, is as well. In addition, the reaction rates are particularly small when CH_3^+ transfer is nearly thermoneutral, as is the case here.[55]

Thermochemistry of Neutral $(CO)_5MnH$ and $(CO)_5MnCH_3$. The protonation reactions 7 and 9 both yield $(CO)_5Mn^+$ from $(CO)_5MnH$ and $(CO)_5MnCH_3$, respectively. The difference in the proton affinity values for the onsets of these reactions links the heat of formation of the neutral reactants, as given in eq. 23. This can also be expressed as a

$$\Delta H_f^\circ[(CO)_5MnH] = \Delta H_f^\circ[(CO)_5MnCH_3] + (12 \pm 2) \text{ kcal/mol} \qquad (23)$$

difference in the manganese-hydrogen and -methyl bond energies, eq. 24.

$$D[(CO)_5Mn - H] = D[(CO)_5Mn-CH_3] + (5 \pm 2) \text{ kcal/mol} \qquad (24)$$

Reactions 16 and 17 produce the common ion $(CO)_5Mn^-$ from $(CO)_5MnH$ and $(CO)_5MnCH_3$, respectively. Just as with the proton affinity data, these give the difference of the bond energies in the

neutral complexes, eq. 25.

$$3.1\,\text{kcal/mol} \leq D[(CO)_5Mn\text{-}H] - D[(CO)_5Mn\text{-}CH_3] \leq 23.2\,\text{kcal/mol} \quad (25)$$

The bond energy difference of 5 kcal/mol in eq. 24 provides a 5 kcal/mol limit for $EA[(CO)_5Mn]$, which is determined from the zero-energy electron negative ion mass spectra to be between the manganese-hydrogen and -methyl bond energies.

Reaction 5, in which $(CO)_5MnH_2^+$ is produced from reaction of $(CO)_5MnH^+$ with $(CO)_5MnH$, indicates $D[(CO)_5Mn\text{-}H] \leq D[(CO)_5MnH^+\text{-}H]$. This is consistent with the values $D[(CO)_5Mn\text{-}H] = 57$ kcal/mol and $D[(CO)_5MnH^+\text{-}H] = 87$ kcal/mol cited above.

Conclusions

These studies are important in providing quantitative data pertaining to a variety of processes important in catalytic and synthetic organometallic chemistry. These include an understanding of the energetics and electronic changes on oxidative addition of CH_4 and H_2 to a metal center. The addition of CH_4 to $(CO)_5Mn^+$ is endothermic; a substantial amount of energy is required for the electronic excitation necessary to form two σ-bonds to the metal complex. Addition of H_2 to $(CO)_5Mn^+$ is exothermic, with a strong H-H interaction in large part responsible for this difference. We expect these conclusions are generally applicable to oxidative addition to complexes for which the ground state is a singlet.

The dual nature of a transition metal hydride is highlighted by the heterolytic bond energies, $D[(CO)_5Mn^+-H^-] = 201$ kcal/mol and $D[(CO)_5Mn^--H^+] = 318$ kcal/mol; that is, the molecule is both very "hydridic" and very "acidic".

A determination of the difference in the sigma bond energies in the neutral complexes is provided both by the protonation reactions and the reactions with negative ions; the protonation reactions yield $D[(CO)_5Mn-H] = D[(CO)_5Mn-CH_3] + (5 \pm 2)$ kcal/mol. These data are in serious disagreement with the reported values $D[(CO)_5Mn-CH_3] = 31 \pm 3$ kcal/mol[56] and $D[(CO)_5Mn-H] = 57$ kcal/mol.[37] Although these values are based upon thermochemical heats of formation, which require substantial auxiliary data (e.g., heats of vaporization and heat capacities of the metal complexes), it is difficult to assess why these determinations may be in error.

There are only a handful of other transition metal species for which thermochemical data exist for both the hydride and the methyl compound. These include: $D[Co\text{-}H] = 39 \pm 6$ and $D[Co\text{-}CH_3] = 41 \pm 10$ kcal/mol,[57] $\overline{D}(Mo\text{-}H) - \overline{D}(Mo\text{-}CH_3) = 24.5 \pm 1.5$ kcal/mol for $(\eta^5\text{-}C_5H_5)_2MoH_2$ and $(\eta^5\text{-}C_5H_5)Mo(CH_3)_2$, $\overline{D}(W\text{-}H) - \overline{D}(W\text{-}CH_3) = 25.4 \pm 1.4$ kcal/mol for $(\eta^5\text{-}C_5H_5)_2WH_2$ and $(\eta^5\text{-}C_5H_5)_2W(CH_3)_2$, (for which $\overline{D}$ indicates the <u>average</u> bond energy),[19] and $D(Ir\text{-}H) - D(Ir\text{-}CH_3) = 13.6 \pm 4.4$ kcal/mol in the compounds resulting from <u>cis</u> addition of HI and <u>trans</u> addition of CH_3I to <u>trans</u>-$[IrCl(CO)(P(CH_3)_3)_3]$.[20] Both the wide range in magnitude of these data, as well as the diverse nature of the complexes for which they are available, make it clear that the problem of relative metal-hydrogen and -methyl bond energies is only just being probed.

Acknowledgments

This work was supported in part by the United States Department of Energy. A.E.S. would like to thank N.S.F. for a Graduate Fellowship (1976-1979) during which time many of these data were determined.

References and Notes

1. James, B. R. "Homogeneous Hydrogenation"; Wiley-Interscience, New York, 1973. Halpern, J. Accts. Chem. Res. 1970, 3, 386. Collman, J. P.; Roper, W. R. Adv. Organomet. Chem. 1968, 7, 53.
2. Norton, J. R. Accts. Chem. Res. 1979, 12, 139.
3. Cooper, N. J.; Green, M. L. H.; Mahtab, R. J. Chem. Soc., Dalton Trans. 1979, 1557.
4. Muetterties, E. L.; Watson, P. L. J. Am. Chem. Soc. 1978, 100, 6978.
5. Abis, L.; Sen, A.; Halpern, J. J. Am. Chem. Soc. 1978, 100, 2915.
6. Davidson, P. J.; Lappert, M. F.; Pearce, R. Chem. Rev. 1976, 76, 219. Schrock, R. R.; Parshall, G. W. Chem. Rev. 1976, 76, 243.
7. Åkermark, B.; Ljungquist, A. J. Organomet. Chem. 1979, 182, 47.
8. Jones, W. D.; Bergman, R. C. J. Am. Chem. Soc. 1979, 101, 5447.
9. Halpern, J. Pure and Appl. Chem. 1979, 51, 2171.
10. McAlister, D. R.; Erwin, D. K.; Bercaw, J. E. J. Am. Chem. Soc. 1978, 100, 5966.
11. Gell, K. I.; Schwartz, J. J. Am. Chem. Soc. 1978, 100, 3246.
12. Brintzinger, H. H. J. Organomet. Chem. 1979, 171, 337.
13. Johnson, M. D. Accts. Chem. Res. 1978, 11, 57.
14. Romeo, R.; Minniti, D.; Lanza, S. J. Organomet. Chem. 1979, 165, C36.

References (continued)

15. Johnson, R. W.; Pearson, R. G. Inorg. Chem. 1971, 10, 2091.

16. Vaska, L.; Werneke, M. F. Trans. N.Y. Acad. Sci., Series 2 1971, 33, 70.

17. Stevens, A. E.; Beauchamp, J. L. J. Am. Chem. Soc. 1979, 101, 245, in which portions of this work were communicated.

18. Connor, J. A. Top. Curr. Chem. 1977, 71, 71.

19. Calado, J. C. G.; Dias, A. R.; Martinho-Simoes, J. A.; Ribeiro da Silva, M. A. V. J. Organomet. Chem. 1979, 174, 77.

20. Yoneda, G.; Blake, D. M. J. Organomet. Chem. 1980, 190, C71.

21. Beauchamp, J. L. Annu. Rev. Phys. Chem. 1971, 22, 527.

22. Wolf, J. F.; Staley, R. H.; Koppel, I.; Taagepera, M.; McIver, Jr., R. T.; Beauchamp, J. L.; Taft, R. W. J. Am. Chem. Soc. 1977, 99, 5417. All proton affinities are reported relative to $PA(NH_3)$ = 207 ± 2 kcal/mol, for which lower and upper limits of 204 and 208 kcal/mol seem well established: Houle, F. A.; Beauchamp, J. L. J. Am. Chem. Soc. 1979, 101, 4067. Errors in the relative scale of proton affinities are estimated to be ± 0.2 kcal/mol.

23. Davison, A.; Faller, J. W. Inorg. Chem. 1967, 6, 845.

24. Closson, R. D.; Kozikowski, J.; Coffield, T. H. J. Org. Chem. 1957, 22, 598. Hieber, W.; Wagner, G. Justus Liebigs Ann. Chem. 1958, 618, 24.

25. Woodin, R. L.; Foster, M. S.; Beauchamp, J. L. J. Chem. Phys. 1980, 72, 4223.

References (continued)

26. Saalfeld, F. E.; McDowell, M. V.; DeCorpo, J. J.; Berry, A. D.; MacDiarmid, A. G. Inorg. Chem. 1973, 12, 48.

27. Mays, M. J.; Simpson, R. N. F. J. Chem. Soc. (A) 1967, 1936.

28. Corderman, R. R., Ph.D. Thesis, California Institute of Technology, 1976.

29. Bartness, J. E.; McIver, Jr., R. T. in Bowers, M. T., Ed., "Gas-Phase Ion Chemistry", Academic Press: New York, 1978.

30. Calculated from the bond energies $D[CH_3\text{-}I] = 55.5 \pm 3$ kcal/mol and $D[CH_3\text{-}Cl] = 81 \pm 5$ kcal/mol: Darwent, B. de B, "Bond Dissociation Energies in Simple Molecules", NSRDS-NBS 31, 1970; $IP[CH_3] = 9.84$ eV: Houle, F. A.; Beauchamp, J. L. J. Am. Chem. Soc. 1979, 101, 4067; and the electron affinity data given in ref. 29.

31. Foster, M. S.; Beauchamp, J. L. J. Am. Chem. Soc. 1975, 97, 4808.

32. Allison, J.; Ridge, D. P. J. Am. Chem. Soc. 1979, 101, 4998.

33. Foster, M. S.; Beauchamp, J. L. J. Am. Chem. Soc. 1975, 97, 4814.

34. Corderman, R. R.; Beauchamp, J. L. Inorg. Chem. 1976, 15, 665.

35. Winters, R. E.; Kiser, R. W. J. Phys. Chem. 1965, 69, 1618. Saalfeld, F. E.; McDowell, M. V.; Gondal, S. K.; MacDiarmid, A. G. J. Am. Chem. Soc. 1968, 90, 3684. Dunbar, R. C.; Ennever, J. F.; Fackler, Jr., J. P. Inorg. Chem. 1973, 12,

References (continued)

2734. Blake, M. R.; Garnett, J. L.; Gregor, I. K.; Wild, S. B. Org. Mass Spectrom. 1978, 13, 20. Blake, M. R.; Garnett, J. L.; Gregor, I. K.; Wild, S. B.; J. Chem. Soc., Chem. Commun. 1979, 496. Lausarot, P. M.; Vaglio, G. A.; Valle, M. Inorg. Chim. Acta 1979, 35, 227.

36. Stevens, A. E.; Beauchamp, J. L. J. Am. Chem. Soc., accepted for publication.

37. Connor, J. A., private communication.

38. Halpern, J., private communication, based on data reported in Sweany, R. L.; Halpern, J. J. Am. Chem. Soc. 1977, 99, 8335.

39. Raffenetti, R. C.; Ruedenberg, K. J. Chem. Phys. 1973, 59, 5978.

40. Kebarle, P. Ann. Rev. Phys. Chem. 1977, 28, 445.

41. Hay, P. J., private communication.

42. Davison, A.; McFarlane, W.; Pratt, L.; Wilkinson, G. J. Chem. Soc. 1962, 3653.

43. Trogler, W. C. J. Am. Chem. Soc. 1979, 101, 6459.

44. Vogt, J.; Williamson, A. D.; Beauchamp, J. L. J. Am. Chem. Soc. 1978, 100, 3478.

45. Bowers, M. T.; Shuying, L.; Kemper, P.; Stradling, R.; Webb, H.; Aue, D. H.; Gilbert, J. R.; Jennings, K. R. J. Am. Chem. Soc. 1980, 102, 4830.

46. Lias, S. G.; Shold, D. M.; Ausloos, P. J. Am. Chem. Soc. 1980, 102, 2540.

References (continued)

47. Pensak, D. A.; McKinney, R. J. Inorg. Chem. 1979, 18, 3407. Elian, M.; Hoffmann, R. Inorg. Chem. 1975, 14, 1058. Burdett, J. K. J. Chem. Soc., Faraday Trans. 2, 1974, 70, 1599.

48. Hieber, W.; Wagner, G. Z. Naturforschg. 1958, 13b, 339.

49. Dunbar, R. C.; Hutchinson, B. B. J. Am. Chem. Soc. 1974, 96, 3816.

50. Frenz, B. A.; Ibers, J. A. Inorg. Chem. 1972, 11, 1109.

51. Huber, H.; Kündig, E. P.; Ozin, G. A.; Poë, A. J. J. Am. Chem. Soc. 1975, 97, 308.

52. Lifshitz, C.; Tiernan, T. O.; Hughes, B. M. J. Chem. Phys. 1973, 59, 3182.

53. Hay, P. J.; Frieser, B. S.; Beauchamp, J. L., private communication.

54. Engelking, P. C.; Lineberger, W. C. J. Am. Chem. Soc. 1979, 101, 5569.

55. Olmstead, W. N.; Brauman, J. I. J. Am. Chem. Soc. 1977, 99, 4219.

56. Brown, D. L. S.; Connor, J. A.; Skinner, H. A. J. Organomet. Chem. 1974, 81, 403.

57. Armentrout, P. B.; Beauchamp, J. L. J. Am. Chem. Soc. 1980, 102, 1736.

Chapter III

Determination of Metal Hydrogen Bond Dissociation Energies by the Deprotonation of Transition Metal Hydride Ions: Application to MnH^+

DETERMINATION OF METAL HYDROGEN BOND DISSOCIATION ENERGIES BY THE DEPROTONATION OF TRANSITION METAL HYDRIDE IONS: APPLICATION TO MnH^+

Amy E. Stevens and J. L. Beauchamp

Arthur Amos Noyes Laboratory of Chemical Physics[†],

California Institute of Technology, Pasadena, California 91125, USA

Ion cyclotron resonance trapped ion techniques are used to examine the kinetics of proton transfer from MnH^+ (formed as a fragment ion from $HMn(CO)_5$ by electron impact) to bases of varying strength. Deprotonation is rapid with bases whose proton affinity exceeds 196 ± 3 kcal mol^{-1}. Using this value for PA (Mn) yields the homolytic bond dissociation energy D (Mn^+-H) = 53 ± 3 kcal mol^{-1}.

[†]Contribution No. 6328.

1. Introduction

Transition metal hydrides are of considerable theoretical interest since they are the simplest species which can be studied to better understand the nature and energetics of sigma bonding in transition metal compounds [1-3]. Experimental interest in these species results, for example, from their observation in spectra of stellar atmospheres [3,4], their importance as reactive intermediates in homogeneous and heterogeneous catalysis [5], their use in hydrogen storage systems [6], and their involvement in schemes for interconversion of H_2, O_2 and H_2O [7]. Despite this, very little information is available concerning metal hydrogen bond strengths. Several new approaches to this problem have been explored in our laboratories [8-10].

In the present work we demonstrate that studies of the kinetics of deprotonation of diatomic transition metal hydride ions, reaction 1, in which M = metal and B is a neutral n-donor base, can be used to

$$MH^+ + B \rightarrow BH^+ + M \qquad (1)$$

quantify the base strengths (proton affinities) of metal atoms and provide metal hydrogen homolytic bond dissociation energies, $D^0[M^+\text{-}H]$. The energetics of B and BH^+ are well characterized for a wide range of n-donor bases [11-12]. An examination of process 1 thus links the heats of formation of M and MH^+. Other examples where this experimental methodology has been successfully applied include determination of the heats of formation of CF_2 [13] and $(CH_3)_2SiCH_2$ [14] by examining deprotonation reactions of the corresponding conjugate acids.

2. Experimental

The experimental techniques and instrumentation for ion cyclotron resonance spectroscopy (icr) have been described in detail [15]. All experiments were performed at ambient temperature (~ 25°C in the icr cell). Pressures were measured using a Schulz-Phelps gauge calibrated at higher pressures against a Model 90H1-MKS Instrument capacitance manometer. Estimated accuracy of pressure measurements is ±20%, which determines the accuracy of rate constants.

$HMn(CO)_5$ was prepared as described in the literature and purified by degassing the sample held at -78° until no impurities were detected in the mass spectrum [16]. This species slowly decomposes to yield trace amounts of H_2, CO, CO_2, and $Mn_2(CO)_{10}$, which do not interfere with the present experiments. Formaldehyde was prepared by thermal cracking of the trimer and purified by vacuum distillation. All other samples were obtained from commercial sources and used as supplied except for degassing at liquid nitrogen temperature.

3. Results and Discussion

Manganese hydride ion is observed as a fragment in the mass spectrum of $HMn(CO)_5$, comprising 10% of the total ion abundance at 70 eV. This species reacts with the parent neutral ($k = 1.1 \times 10^{-9}$ cm^3 $molec^{-1}$ s^{-1}) as indicated in equation 2. In the presence of a sufficiently

$$MnH^+ + HMn(CO)_5 \rightarrow Mn_2(CO)_4^+ + CO + H_2 \qquad (2)$$

strong n-donor base the disappearance of MnH^+ is more rapid. This is

shown for the case of isopropyl cyanide in Figure 1. By taking the log of the ratio of the MnH^+ signal intensity with and without added base (Figure 2), the rate of the proton transfer reaction 3 is determined to

$$MnH^+ + (CH_3)_2CHCN \rightarrow (CH_3)_2CHCNH^+ + Mn \qquad (3)$$

be 1.5×10^{-9} cm^3 $molec^{-1}$ s^{-1}. Continuous ejection of MnH^+ leads to a decrease in the abundance of $(CH_3)_2CHCNH^+$ which quantitatively accounts for the removal of MnH^+ and confirms the proton transfer process.

Measured proton transfer rates are summarized in Table 1, and compared to the calculated collision rates using the ADO analysis of Bowers and coworkers [17]. These quantities are illustrated graphically in Figure 3 as a function of the proton affinity of the organic base. All proton affinity data are relative to $PA(NH_3)$ = 207.0 kcal mol^{-1}. This value is the subject of controversy, but almost certainly is between the limits of 204 and 209 kcal mol^{-1} [12]; this is the major uncertainty in PA(Mn).

Where proton transfer is thermoneutral, proton transfer is expected to occur at about half the collision frequency. This point is indicated in Figure 3, from which PA(Mn) = 195.5 ± 2.5 kcal mol^{-1} is taken. Using IP(Mn) = 7.43 eV [18], a metal hydrogen homolytic bond energy $D^0(Mn^+\text{-}H)$ = 53 ± 3 kcal mol^{-1} is derived. This is compared with other recently determined transition metal hydrogen bond dissociation energies, $D^0(M^+\text{-}H)$, in Table 2 [8,9,19].

Several complications in these experiments deserve comment. Electronically excited transition metal ions are formed in reasonable

FIGURE 1. Variation of the abundance of MnH^+ with time, following a 70 eV, 10 msec. electron pulse. The upper curve depicts the decay of MnH^+ in the presence of 1.5×10^{-7} Torr $HMn(CO)_5$. The lower curve illustrates the increased rate of decay when 1.7×10^{-7} Torr of $(CH_3)_2CHCN$ is added.

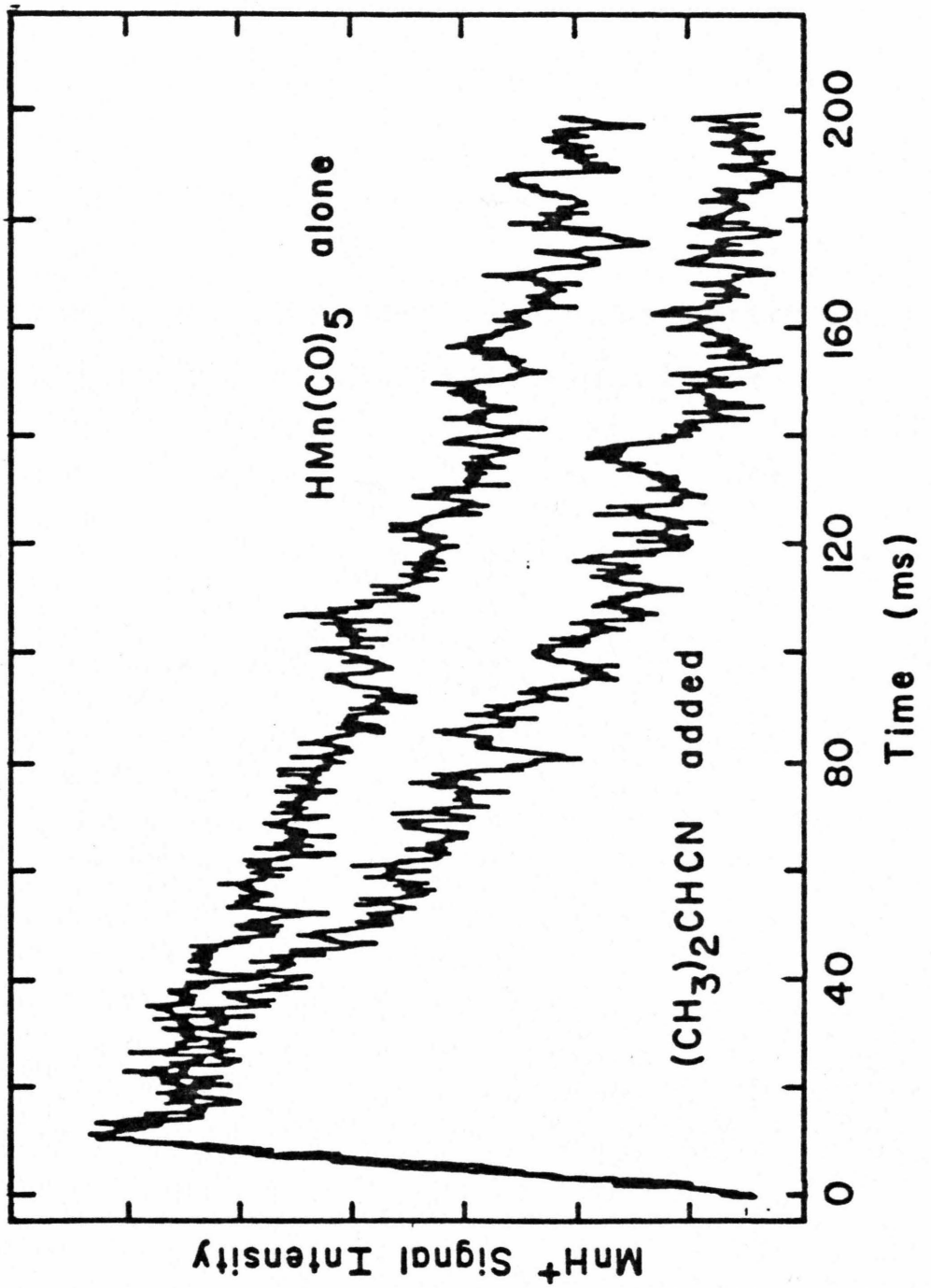
MnH+ Signal Intensity
0
40
80
120
160
200
Time (ms)
HMn(CO)5 alone
(CH3)2CHCN added

FIGURE 2. Ratio of the MnH^+ signal with and without added $(CH_3)_2CHCN$ as a function of time. Conditions are as in Figure 1.

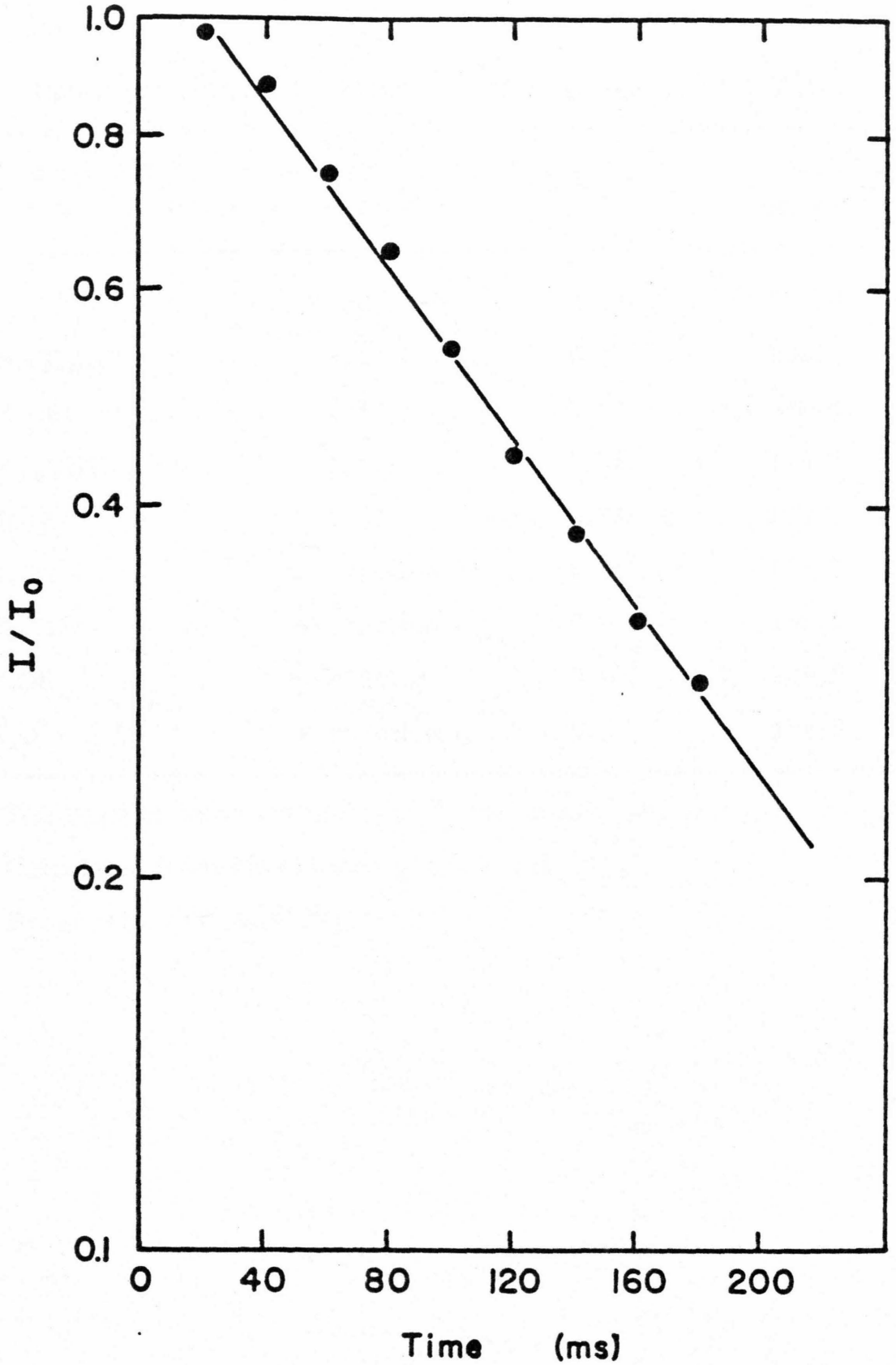
1.0
0.8
0.6
0.4
0.2
0.1
I/I₀
0
40
80
120
160
200
Time (ms)

Table 1

Rate Constants for Reaction of Proton Acceptors with MnH^+

Proton Acceptor B	$k \times 10^9$, [a] $cm^3\,molec^{-1}\,s^{-1}$	k/k_{ADO} [b]	PA(B) [c] kcal mol^{-1}
NH_3	1.3	0.74	207.0
$(CH_3CH_2)_2O$	1.1	0.75	202.1
$(CH_3)_2CO$	1.1	0.50	198.6
$(CH_3)_2CHCN$	1.5	0.58	196.9
$(CH_3)_2O$	0.31	0.21	194.8
CH_3CN	no reaction	0.0	191.7
CH_3CHO	no reaction	0.0	189.1
CH_3OH	no reaction	0.0	186.9
CH_2O	no reaction	0.0	179.3

a) The limit of detection is $k = 10^{-11}$ cm^3 $molec^{-1}$ s^{-1}.

b) Calculated from the formula given in ref. [17].

c) From refs. [11] and [12].

FIGURE 3. Rate constants as a function of proton affinity of B for the reaction $MnH^+ + B \rightarrow BH^+ + Mn$. The open circles are the measured rate constants. Closed circles are the measured rate constants divided by the encounter rate, k/k_{ADO}.

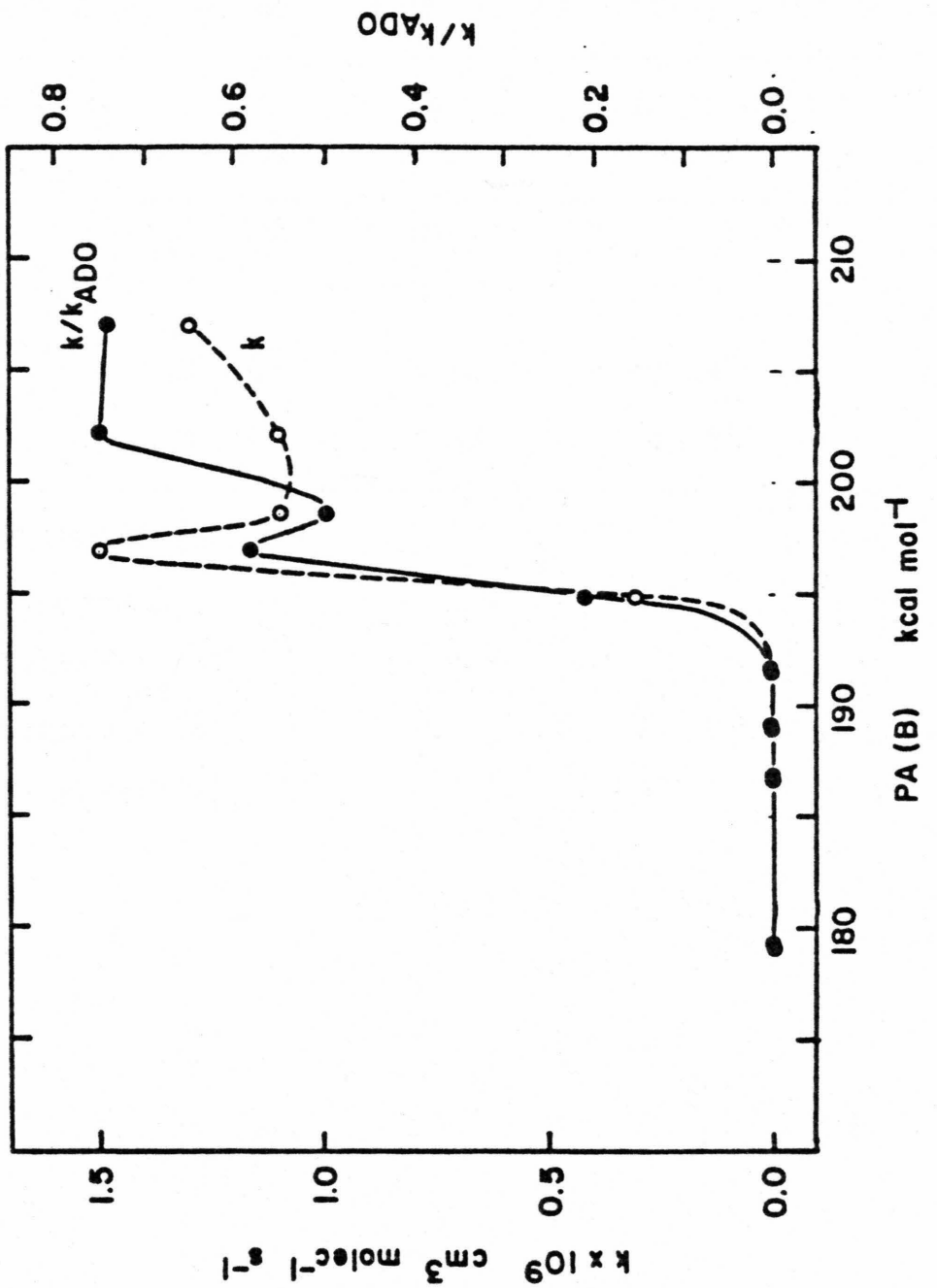
k/kADO
0.8
0.6
0.4
0.2
0.0
k/kADO
k
1.5
1.0
0.5
0.0
k x 10⁹ cm³ molec⁻¹ s⁻¹
180
190
200
210
PA (B) kcal mol⁻¹

Table 2

Proton Affinities, Ionization Potentials, Metal-Hydrogen and Metal-Methyl Homolytic Bond Energies of Transition Metal Atoms

Metal M	PA(M) kcal mol^{-1}	IP(M)[a] eV	$D^0(M^+-H)$ kcal mol^{-1}	$D^0(M^+-CH_3)$ kcal mol^{-1}
Mn	196 ± 3[b]	7.43	53 ± 3[b]	$> 48 \pm 3$[b]
Fe				62 ± 6[c]
Co	184 ± 5[d]	7.86	52 ± 4[d]	61 ± 4[d]
Ni	181 ± 2[e]	7.63	43 ± 2[e]	

a) From ref. [18].

b) This work.

c) From ref. [19].

d) From ref. [8].

e) From ref. [9].

abundance in the fragmentation of organometallic compounds. These species exhibit enhanced reactivity. In the mixture of formaldehyde with $HMn(CO)_5$, addition of the organic base leads to an increase in the MnH^+ signal which double resonance experiments indicate to come from Mn^+, reaction 4. Continuous ejection of Mn^+ eliminates this

$$Mn^+ + CH_2O \rightarrow MnH^+ + HCO \qquad (4)$$

contribution, and no increased decay of the MnH^+ signal is observed with added CH_2O ($k < 10^{-11}$ cm^3 molec^{-1} s^{-1}). Using the above bond energy, reaction 4 is endothermic by ~ 37 kcal mol^{-1}. The lowest excited state of Mn^+ with sufficient energy to render process 4 exothermic is a ^5D at 1.78 eV (41 kcal mol^{-1}) [18].

Proton transfer is generally a facile process. In the deprotonation of MnH^+ with sufficiently strong bases this is the only observed reactive pathway. With weak bases the protonation is endothermic, and other reactions may be observed. In the case of CH_3CHO, for example, MnH^+ decays when the neutral base is added to the system, even though no proton transfer is observed. Process 5 is identified by double resonance, and a rate constant of 2.8×10^{-10} cm^3 molec^{-1} s^{-1}

$$MnH^+ + CH_3CHO \rightarrow MnCH_3^+ + H_2 + CO \qquad (5)$$

is obtained from an analysis of the temporal behavior of ion concentrations. The neutral products are not identified; the only reasonable alternate product in reaction 5 is CH_2O, which has nearly the same heat of formation as H_2 and CO.

The decarbonylation of aldehydes has been observed with other transition metal complexes [20] and atomic ions [21]. The usual process yields the metal carbonyl, via the scheme presented in Figure 4. In the case of MnH^+ the presence of a hydrogen on the metal center allows for the reductive elimination of H_2, presumably before the methyl group transfers to the metal center, as is also shown in Figure 4. As a result, the product $MnCH_3^+$ is observed instead of the carbonyl. Using the derived MnH^+ bond energy, reaction 5 indicates $D^0(Mn^+\text{-}CH_3) \geq 48 \pm 3$ kcal mol^{-1}. This is in keeping with other reported metal-methyl bond energies, which are given in Table 2.

The long time scale of trapped ion icr experiments makes necessary the consideration that vibrationally or electronically excited ions will relax radiatively; this phenomenon has been observed indirectly in a number of other experiments [22-25]. A major concern here is with the possibility that excited species participate in the observed deprotonation reactions. For an inhomogeneous ion population with varying reactivity, a non-linear log plot (of the type shown in Figure 2) would be obtained. In no instance is this observed, and the involvement of excited MnH^+ is ruled out.

It is interesting to compare $D(Mn^+\text{-}H)$ to the bond energies in related neutral molecules. For main group hydrides, the bond energy in the ion is typically 10-15 kcal mol^{-1} stronger than in the isoelectronic neutral [11]. Our data would indicate that $D^0(Cr\text{-}H) \leq 53$ kcal mol^{-1}. In addition, combining our data with IP(MnH) would yield the bond energy $D^0(Mn\text{-}H)$; this ionization potential has not been reported.

FIGURE 4. Mechanism of decarbonylation of aldehydes by transition metal ions, and mechanism of decarbonylation by a transition metal hydride ion.

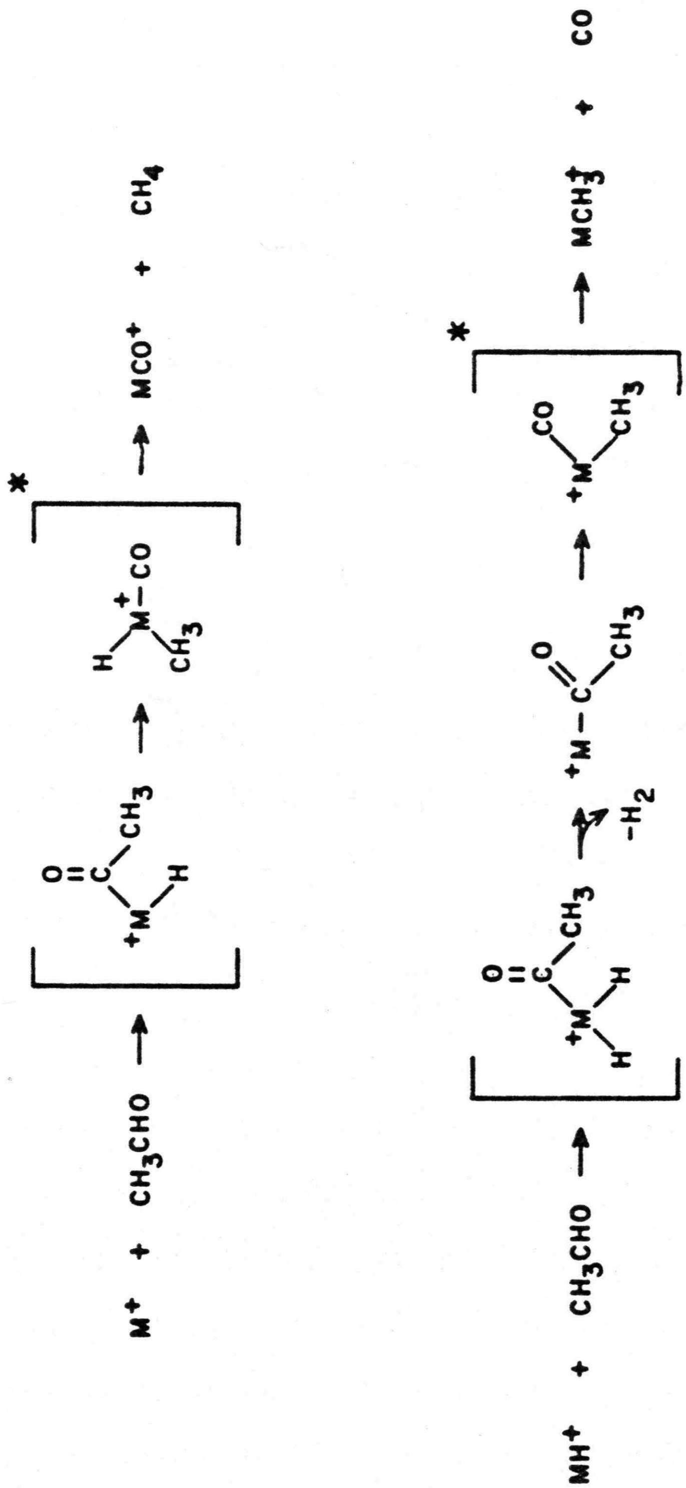
M⁺ + CH3CHO
MCO⁺ + CH4
MH⁺ + CH3CHO
-H2
MCH3⁺ + CO

A consideration of the electronic structure of MnH [1] indicates the electron lost on ionization is an s-p hybrid somewhat antibonding with respect to the Mn-H bond. This suggests IP(MnH) < IP(Mn), from which it follows that $D^0(Mn\text{-}H) < D^0(Mn^+\text{-}H) = 53$ kcal mol^{-1}. Gaydon [26] has estimated $D^0(Cr\text{-}H) = 66 \pm 12$ kcal mol^{-1} and $D^0(Mn\text{-}H) = 55 \pm 7$ kcal mol^{-1}, by using a linear Birge-Sponer extrapolation of the v = 0-2 vibrational levels for these molecules. This extrapolation appears to be seriously in error for transition metal hydrides, which is not unexpected considering the major assumptions involved in its use.

4. Conclusion

The present work demonstrates that studies of the kinetics of deprotonation reactions of metal hydride ions form the basis of an experimental method for the determination of metal atom base strengths and metal-hydrogen bond dissociation energies. This complements other techniques, which include protonation of the neutral metal, an analysis of thresholds for endothermic reactions, and extrapolations of spectroscopic data.

The ion MnH^+ is isoelectronic with CrH and very likely has the same $^6\Sigma^+$ ground state [27]. Deprotonation yields the ^6S ground state of the atom derived from the configuration s^2d^5. The reaction is thus expected to occur on a single electronic surface to yield ground state products. This may contribute to the almost ideal behavior of the MnH^+ system, and is not unexpected for many other metal hydride ions.

5. Acknowledgment

This work was supported in part by the United States Department of Energy.

References

[1] P. S. Bagus and H. F. Schaefer III, J. Chem. Phys. 58 (1973) 1844.

[2] J. Demuynck and H. F. Schaefer III, J. Chem. Phys. 72 (1980) 311, and references therein.

[3] P. H. Scott and W. G. Richards, Molecular Spectroscopy 4 (1976) 70.

[4] W. Weltner, Jr., Ber. Bunsenges. Phys. Chem. 82 (1978) 80.

[5] B. R. James, Homogeneous Hydrogenation (Wiley-Interscience, New York, 1973). H. F. Schaefer III, Acc. Chem. Res. 10 (1977) 287, and references therein.

[6] F. R. Kalhammer and T. R. Schneider, Annu. Rev. Energy 1 (1976) 311.

[7] T. Yoshida, T. Okana and S. Otsuka, J. Am. Chem. Soc. 102 (1980) 5966.

[8] P. B. Armentrout and J. L. Beauchamp, J. Am. Chem. Soc. 102 (1980) 1736.

[9] P. B. Armentrout and J. L. Beauchamp, Chem. Phys. 50 (1980) 37.

[10] A. E. Stevens and J. L. Beauchamp, J. Am. Chem. Soc., in press.

[11] J. F. Wolf, R. H. Staley, I. Koppel, M. Taagepera, R. T. McIver, Jr., J. L. Beauchamp and R. W. Taft, J. Am. Chem. Soc. 99 (1977) 5417.

[12] F. A. Houle and J. L. Beauchamp, J. Am. Chem. Soc. 101 (1979) 4067.

References (continued)

[13] J. Vogt and J. L. Beauchamp, J. Am. Chem. Soc. 97 (1975) 6682.

[14] W. J. Pietro, S. K. Pollack and W. J. Hehre, J. Am. Chem. Soc. 101 (1979) 7126.

[15] J. L. Beauchamp, Annu. Rev. Phys. Chem. 22 (1971) 527. T. B. McMahon and J. L. Beauchamp, Rev. Sci. Instr. 43 (1972) 509.

[16] H. Davison and J. W. Faller, Inorg. Chem. 6 (1967) 845.

[17] T. Su and M. T. Bowers, Int. J. Mass Spectrom. Ion Phys. 12 (1973) 347.

[18] C. E. Moore, Atomic Energy Levels, Vol. 2 (Nat. Bur. Std., Washington, 1971) pp. 27, 78, 97.

[19] J. Allison and D. P. Ridge, J. Organometal. Chem. 99 (1975) C11.

[20] R. R. Corderman and J. L. Beauchamp, J. Am. Chem. Soc. 98 (1976) 5700.

[21] P. B. Armentrout, L. F. Halle, W. Crowe and J. L. Beauchamp, unpublished results.

[22] P. B. Armentrout, D. W. Berman and J. L. Beauchamp, Chem. Phys. Lett. 53 (1978) 255.

[23] R. L. Woodin and J. L. Beauchamp, Chem. Phys. 41 (1979) 1.

[24] R. L. Woodin, M. S. Foster and J. L. Beauchamp, J. Chem. Phys. 72 (1980) 4223.

[25] J. M. Jasinski and J. I. Brauman, Chem. Phys. Lett., submitted for publication.

References (continued)

[26] A. G. Gaydon, Dissociation Energies and Spectra of Diatomic Molecules (Chapman and Hall, London, 1968) pp. 269, 276.

[27] R. J. Van Zee, T. C. DeVore and W. Weltner, Jr., J. Chem. Phys. 71 (1979) 2051, and references therein.

Chapter IV

Photoionization Mass Spectrometry of $(CO)_5MnR$, R = H, CH_3, CH_2F, CHF_2, and CF_3. Determination of the Relative Metal-Hydrogen and Metal-Carbon Bond Energies $D[(CO)_5Mn\text{-}R]$, the Metal-Carbene Bond Energies $D[(CO)_5Mn^+\text{-}CXY]$, X, Y = H, F and the Fluoride and Hydride Affinities, $D[(CO)_5MnCXY^+\text{-}X^-]$.

Photoionization Mass Spectrometry of $(CO)_5MnR$, R = H, CH_3, CH_2F, CHF_2, and CF_3. Determination of the Relative Metal-Hydrogen and Metal-Carbon Bond Energies $D[(CO)_5Mn-R]$, the Metal-Carbene Bond Energies $D[(CO)_5Mn^+-CXY]$, X, Y = H, F and the Fluoride and Hydride Affinities, $D[(CO)_5MnCXY^+-X^-]$

Amy E. Stevens, D. Wayne Berman, and J. L. Beauchamp

Contribution No. 6329 from the Arthur Amos Noyes Laboratory of Chemical Physics, California Institute of Technology, Pasadena, California 91125.

Abstract

Photoionization mass spectrometry is utilized to measure the ionization potentials and selected fragment ion appearance potentials of $(CO)_5MnR$ where R = H, CH_3, CH_2F, CHF_2 and CF_3. A comparison of the appearance potential of $(CO)_5Mn^+$ from all five species yields the metal-carbon bond dissociation energies relative to the metal-hydrogen bond dissociation energy with no additional thermochemical data. Using the literature value $D^0[(CO)_5Mn-H]$ = 57 kcal/mol gives $D^0[(CO)_5Mn-R]$ = 44, 32, 33, and 42 kcal/mol, respectively. Fragmentation thresholds for the metal carbene fragment ions $(CO)_5MnCXY^+$ where X, Y = H or F are analyzed to yield the fluoride and hydride affinities of these species. Ion cyclotron resonance spectroscopy is used to examine hydride and fluoride transfer reactions involving these carbenes to corroborate the photoionization data. The carbene bond dissociation energies $D^0[(CO)_5Mn^+-CXY]$ decrease from 104 to 98 to 82 kcal/mol with successive substitution of F for H.

Introduction

Any discussion of processes such as oxidative addition, reductive elimination, or migratory insertion, which are elementary steps in complex catalytic transformations, has been hampered by an almost complete lack of thermochemical characterization of organometallic complexes. Accurate thermochemical data would greatly enhance our understanding of processes such as hydrogenation, hydroformylation, Zeigler-Natta polymerization, olefin metathesis, and carbonylation, and aid in the design of selective catalyst systems for carrying out these transformations.

The use of indirect spectral evidence and, more generally, structure-energy relationships to rationalize and correlate observed patterns of reactivity has met with some success but may have its limitations in application to organometallic systems. All too often the nebulous concept of "stability" is substituted for a quantitative knowledge of bond enthalpies and activation energies. An example is afforded by comparison of transition metal perfluoroalkyl, alkyl, and hydride complexes. Perfluoroalkyls decompose at much higher temperatures, and are more stable with respect to oxidation than their alkyl analogues.[1] Reactivity patterns of these compounds vary; for $(CO)_5MnCH_3$, ΔH = -12.6 kcal/mol is reported for reaction 1; the reaction

$$(CO)_5MnR + CO \rightarrow (CO)_5MnC(O)R \qquad (1)$$

is reversible at room temperature.[2] Only the reverse, decarbonylation, is observed for R = CF_3.[3,4] The formyl complex (R = H) has not been

detected, but is the postulated intermediate in the rapid reaction (0°) of acetic [^{13}C] formic anhydride with $Na^+[(CO)_5Mn^-]$ to yield ^{13}CO substituted $(CO)_5MnH$.[5] These patterns of reactivity, also apparent with other complexes, have led to the hypothesis that the bond energies decrease in the order $D[(CO)_5Mn\text{-}H] > D[(CO)_5Mn\text{-}CF_3] > D[(CO)_5Mn\text{-}CH_3]$. These conclusions are supported by the proton nmr of $(CO)_5MnCH_3$, $(CO)_5MnCH_2F$, and $(CO)_5MnCHF_2$, in which an increased metal-carbon bond order is postulated to account for the large downfield shift of the alkyl hydrogens on increasing fluorine substitution.[3] A decrease of about 100 cm^{-1} in the carbon-fluorine stretching frequencies in $(CO)_5MnCF_3$ as compared to the trifluoromethyl halides is taken as evidence of a π interaction strengthening the $(CO)_5Mn\text{-}CF_3$ bond relative to $D[(CO)_5Mn\text{-}CH_3]$.[6] Finally, structural data in a number of complexes indicates metal-perfluoroalkyl bonds are consistently slightly shorter than the metal-alkyl bonds.[7]

Similar arguments have been applied to a discussion of heteroatom "stabilized" metal carbene complexes as compared to the carbenes which contain only C and H (alkylidene complexes).[8]

In the past several years some data have been reported which provide metal-alkyl and metal-hydride bond strengths.[9-16] Determination of metal-carbene bond energies is very limited.

Connor has reported values for the bond energies for the pentacarbonylmanganese derivatives $D[(CO)_5Mn\text{-}H]$ = 57 kcal/mol, $D[(CO)_5Mn\text{-}CF_3]$ = 37 kcal/mol, and $D[(CO)_5Mn\text{-}CH_3]$ = 33 kcal/mol, derived from thermochemical heats of formation, from reaction calorimetry.[12] Halpern reports a value $D[(CO)_5Mn\text{-}H]$ = 64 kcal/mol,

determined by the solution kinetics of H atom transfer to α-methyl styrene.[14] Studies in these laboratories of the gas-phase protonation reactions of $(CO)_5MnH$ and $(CO)_5MnCH_3$ indicate that $D[(CO)_5Mn\text{-}H] = D[(CO)_5Mn\text{-}CH_3] + 5 \pm 2$ kcal/mol.[16]

Electron impact and photoionization mass spectrometry (PIMS) can be used with varying degrees of success to provide accurate heats of formation and bond dissociation energies for organometallic neutrals and ions. Of the two techniques the latter is greatly preferred in terms of favorable threshold laws for ionization, greater sensitivity and higher energy resolution. A noteworthy example of previous studies is the PIMS investigation of $(CO)_5Fe$, which has provided the ionization potential $IP[(CO)_5Fe] = 7.98 \pm 0.01$ eV, and the appearance potentials (AP) of each of the fragments resulting from loss of CO, including $AP[Fe^+] = 14.03 \pm 0.1$ eV.[17] This can be compared to $AP[Fe^+] = 13.79 \pm 0.1$ eV calculated from the heats of formation of $(CO)_5Fe$,[9] CO, and Fe^+. By contrast, electron impact thresholds of 14.7 to 16.1 eV have been reported for Fe^+ from $(CO)_5Fe$.[17] Clearly, PIMS studies provide an excellent method for determining ionization potentials as well as appearance potentials of high-energy fragments.

We report here a PIMS study of $(CO)_5MnR$, R = H, CH_3, CH_2F, CHF_2, and CF_3. These data provide the ionization potentials for each of the compounds. Differences in the thresholds for reaction 2 provide

$$(CO)_5MnR + h\nu \rightarrow (CO)_5Mn^+ + R \qquad (2)$$

directly, with no additional thermochemical data, the differences in the neutral bond energies, $D[(CO)_5Mn\text{-}R]$.

Fragmentation of the fluoroalkyls by F loss leads to formation of the carbenes $(CO)_5MnCXY^+$, where X, Y = H or F. Thresholds measured for these processes are combined with other data to calculate the metal carbene bond dissociation energies $D\,[(CO)_5Mn^+\text{-}CXY]$. In addition, the hydride and fluoride affinities of the carbene ions are calculated. The latter results are corroborated by an ion cyclotron resonance investigation of hydride and fluoride transfer reactions involving these species.

Experimental

The California Institute of Technology-Jet Propulsion Laboratory photoionization mass spectrometer used in this study is described in detail elsewhere.[18] The instrument consists of a differentially pumped high-pressure light source, a 1-m normal incidence monochromator (McPherson Model 225), a differentially pumped ionization chamber and a quadrupole mass spectrometer equipped with a Channeltron electron multiplier for ion counting. Light intensities were measured using a sodium salicylate scintillator and a cooled photomultiplier; the relative quantum efficiency of the scintillator was assumed constant over the wavelength region scanned. An osmium-coated grating blazed at 1200 Å and ruled with 1200 lines mm^{-1} was used in first order for the present experiments. Other operating conditions include: resolution, 1 Å; repeller field, 0.5 V cm^{-1}; ion energy for mass analysis, 9.5-10 eV; source temperature, ambient (22° C); sample pressure, typically $1.4 - 3.0 \times 10^{-4}$ Torr. The hydrogen many-line spectrum was utilized for the wavelength range examined (1520 - 1100 Å). Average ion lifetimes prior to mass analysis and detection are in the range 20-30 μsec.

Checks involving systematic variation of pressure and repeller field insured that collision induced dissociation and ion-molecule reactions did not contribute to the observed photoionization efficiency curves.

Fluoride and hydride transfer reactions were examined using the techniques of ion cyclotron resonance spectroscopy.[19] This work

employed an instrument built in our laboratories and utilizes a 15-in electromagnet capable of 23.4 kG maximum field. Standard marginal oscillator detection was employed. All reactions were identified by double resonance techniques; neutrals are not detected.

$(CO)_5MnH$ was prepared by reaction of $Na^+[(CO)_5Mn^-]$ with phosphoric acid.[20] Final purification was effected by pumping in the sample held at -78° until no impurities were observed in the mass spectrum. $(CO)_5MnCH_3$ was prepared by reaction of $Na^+[(CO)_5Mn^-]$ with CH_3I and purified by sublimation;[21] no impurities were observed in the mass spectrum.

$(CO)_5MnC(O)CF_3$,[4] $(CO)_5MnC(O)CHF_2$,[3] and $(CO)_5MnC(O)CH_2F$[3] were prepared by reaction of trifluoroacetic anhydride, difluoroacetyl chloride,[22] and monofluoroacetyl chloride[22] with $Na^+[(CO)_5Mn^-]$. The fluoroalkyls were prepared by repeated decarbonylation of the acyl compounds at 90°, and purified by sublimation.[3,4] The mass spectra of these compounds were checked on the PIMS at 1250 and 1300 Å for the ion $(CO)_6Mn^+$ which is unique to the acyl species; this ion was not detected.

Results

Photoionization Studies. The photoionization efficiency curves for the parent, $(CO)_5Mn^+$, and $(CO)_5Mn(CXY)^+$ ions in the region of their thresholds are illustrated in Figures 1-5. The adiabatic ionization potentials and appearance potentials of the fragments are identified in the Figures and summarized in Table I. Complete breakdown diagrams for these species were not recorded. Loss of CO is a low-energy process in the fragmentation of all the complexes. Photoionization efficiency curves for these and other fragments were not recorded in order to minimize exposure of the instrumentation to the organometallic compounds.

Evaluation of ionization thresholds requires consideration of the contribution of thermal internal energy of the neutral to the dissociation process as well as the possibility of a significant kinetic shift. These phenomena have been discussed in detail in the literature.[23,24]

The initial thermal energy in the parent neutral contributes to the total internal energy of the molecular ion and folds a Maxwellian energy distribution into the threshold curve. The resulting low-energy "tail" on the fragment ionization efficiency curve causes the apparent threshold to be shifted to lower energies by an amount equal to the mean thermal energy content of the parent molecule. These effects have been confirmed for fragmentations in the lower alkanes.[24]

The second effect, that of kinetic shift, is defined as the displacement of the apparent threshold to higher energy by an amount appropriate to raise the dissociation rate to the level at which the fragment ions can be detected. This effect is opposite in direction and

FIGURE 1. Photoionization efficiency curves for the molecular ion and $(CO)_5Mn^+$ in $(CO)_5MnH$.

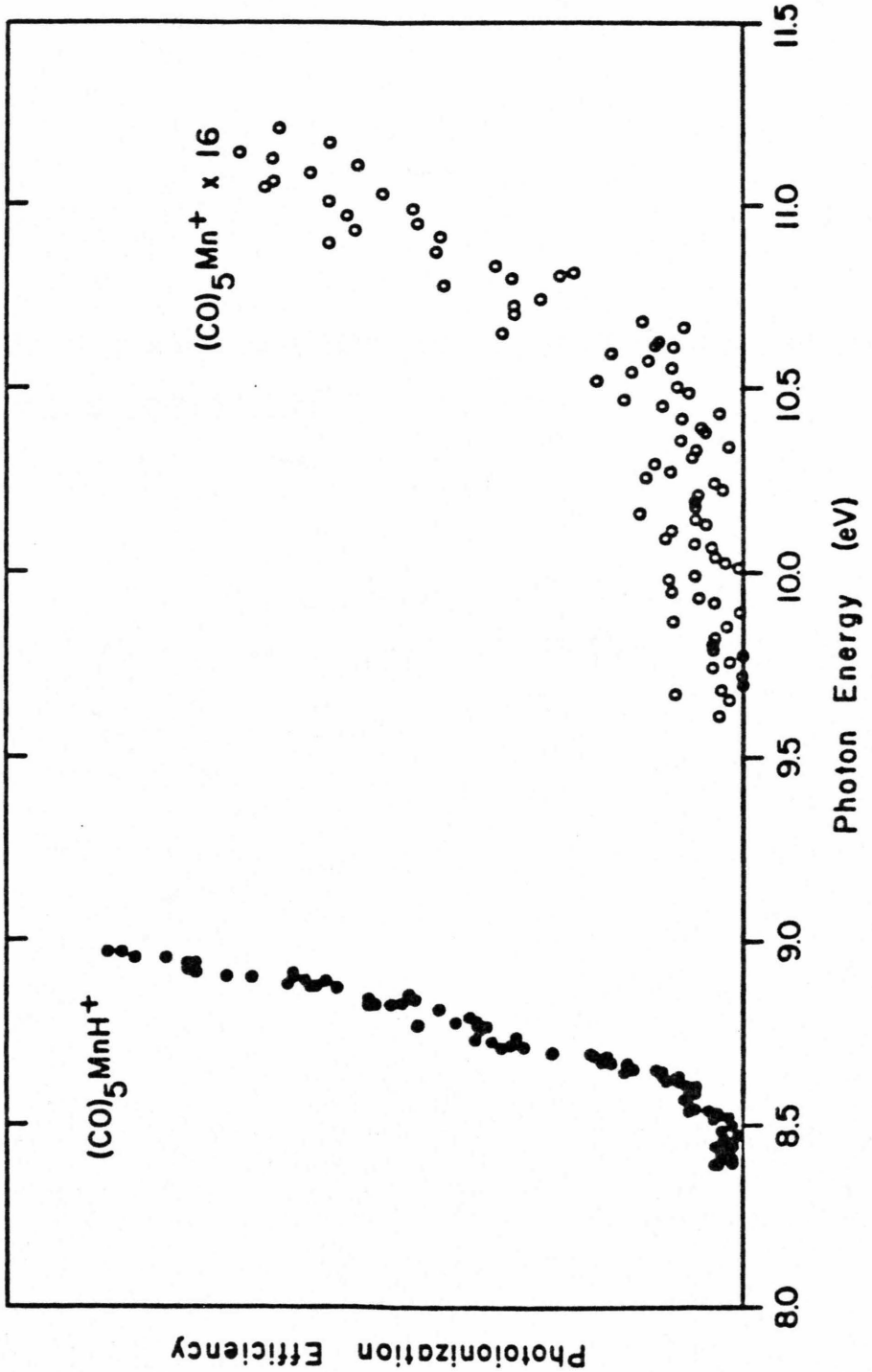
(CO)5MnH+
(CO)5Mn+ x 16
Photoionization Efficiency
8.0
8.5
9.0
9.5
10.0
10.5
11.0
11.5
Photon Energy (eV)

FIGURE 2. Photoionization efficiency curves for the molecular ion and $(CO)_5Mn^+$ in $(CO)_5MnCH_3$.

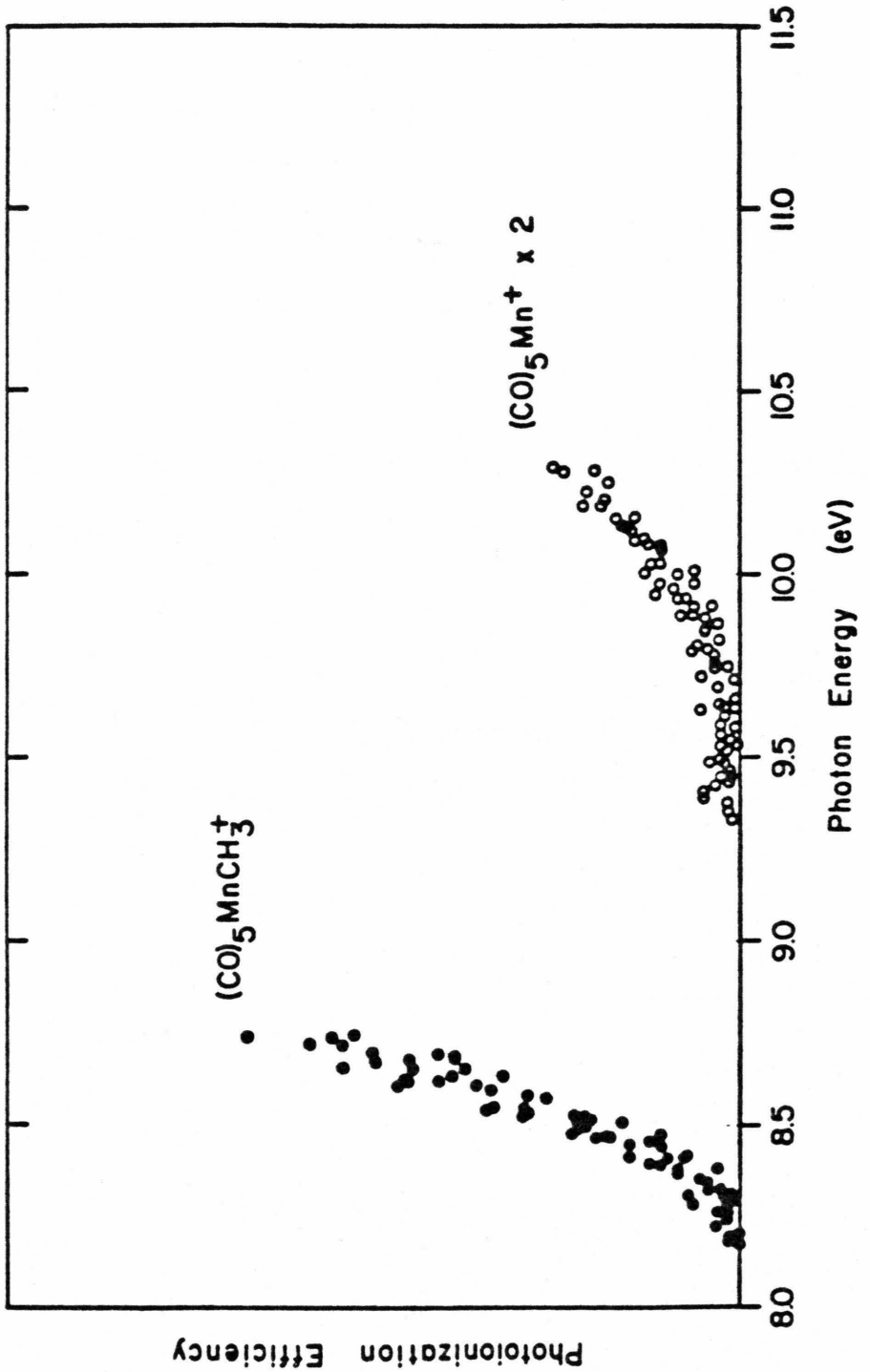
Photoionization Efficiency
8.0
8.5
9.0
9.5
10.0
10.5
11.0
11.5
Photon Energy (eV)
$(CO)_5MnCH_3^+$
$(CO)_5Mn^+$ x 2

FIGURE 3. Photoionization efficiency curves for the molecular ion, $(CO)_5Mn^+$, and $(CO)_5MnCH_2^+$ in $(CO)_5MnCH_2F$.

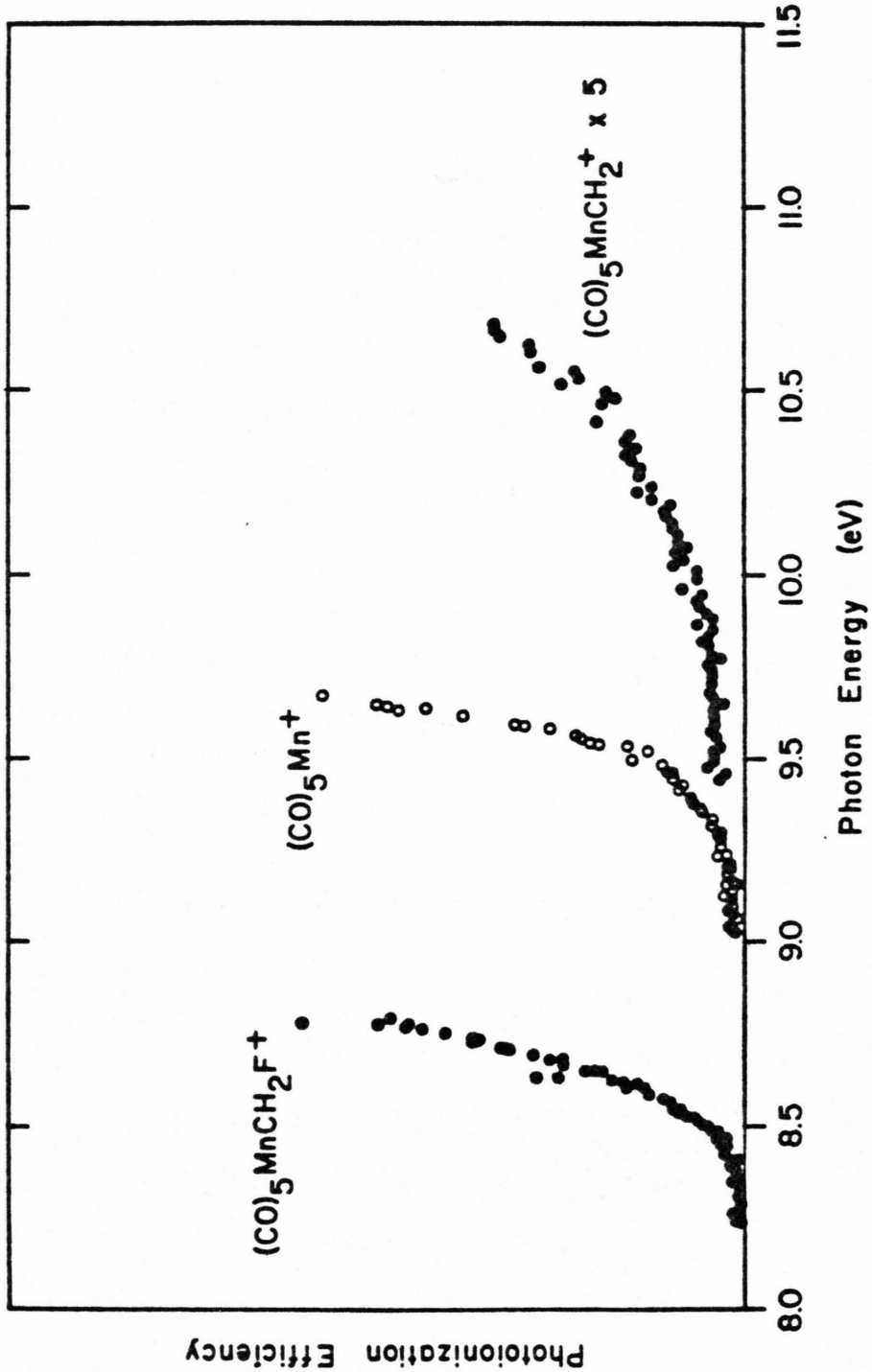
Photoionization Efficiency
8.0
8.5
9.0
9.5
10.0
10.5
11.0
11.5
Photon Energy (eV)
$(CO)_5MnCH_2F^+$
$(CO)_5Mn^+$
$(CO)_5MnCH_2^+$ x 5

FIGURE 4. Photoionization efficiency curves for the molecular ion, $(CO)_5Mn^+$, and $(CO)_5MnCHF^+$ in $(CO)_5MnCHF_2$.

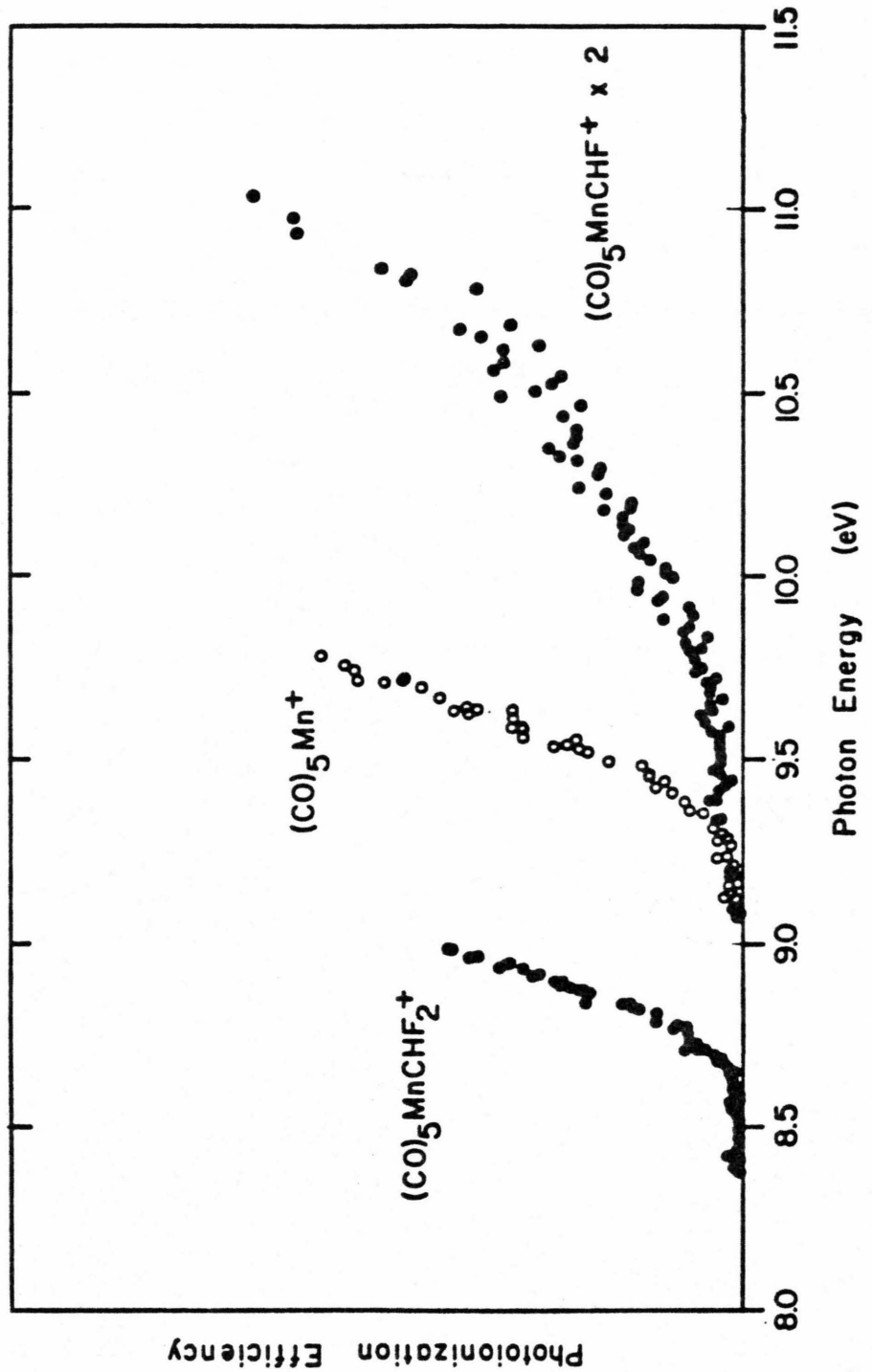
Photoionization Efficiency
8.0
8.5
9.0
9.5
10.0
10.5
11.0
11.5
Photon Energy (eV)
$(CO)_5MnCHF_2^+$
$(CO)_5Mn^+$
$(CO)_5MnCHF^+$ x 2

FIGURE 5. Photoionization efficiency curves for the molecular ion, $(CO)_5Mn^+$, and $(CO)_5MnCF_2^+$ in $(CO)_5MnCF_3$.

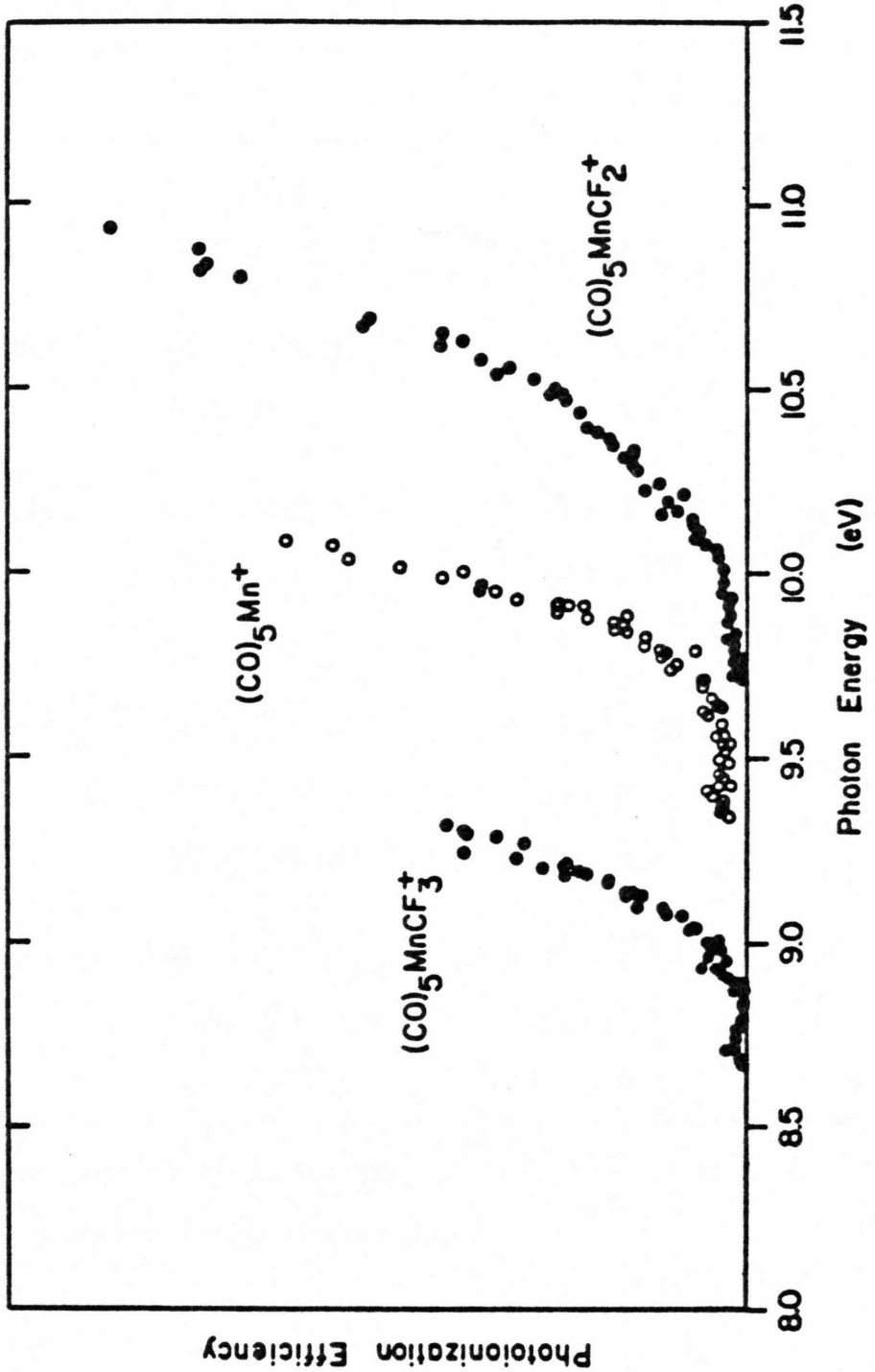
Photoionization Efficiency
8.0
8.5
9.0
9.5
10.0
10.5
11.0
11.5
Photon Energy (eV)
$(CO)_5MnCF_2^+$
$(CO)_5Mn^+$
$(CO)_5MnCF_3^+$

Table I. Ionization Potentials and Appearance Potentials Determined by Photoionization Mass Spectrometry for $(CO)_5MnR$.

Compound	Ion	IP or AP, eV	
$(CO)_5MnH$.	$(CO)_5MnH^+$	8.52 ± 0.03	8.55 ± 0.1[a]
	$(CO)_5Mn^+$	10.3 ± 0.1	
$(CO)_5MnCH_3$	$(CO)_5MnCH_3^+$	8.33 ± 0.03	8.3 ± 0.1[b]
	$(CO)_5Mn^+$	9.75 ± 0.05	
$(CO)_5MnCH_2F$	$(CO)_5MnCH_2F^+$	8.35 ± 0.03	
	$(CO)_5Mn^+$	9.20 ± 0.05	
	$(CO)_5MnCH_2^+$	9.75 ± 0.1	
$(CO)_5MnCHF_2$	$(CO)_5MnCHF_2^+$	8.65 ± 0.03	
	$(CO)_5Mn^+$	9.25 ± 0.05	
	$(CO)_5MnCHF^+$	9.7 ± 0.1	
$(CO)_5MnCF_3$	$(CO)_5MnCF_3^+$	8.90 ± 0.03	8.9 ± 0.1[b]
	$(CO)_5Mn^+$	9.65 ± 0.05	
	$(CO)_5MnCF_2^+$	9.9 ± 0.1	

a) From the photoelectron spectrum.[25]

b) From the photoelectron spectrum.[26]

often comparable in magnitude to the effect of thermal energy, leading to fortuitous cancellation of error. In our instrument the fragmentation rate must be greater than 10^4-10^5 s^{-1} to enable detection of the lowest energy fragment. This is an order of magnitude less than the rates necessary for detection on magnetic sector instruments. For fragmentations analogous to process 2 in systems of similar size, kinetic shift effects have been calculated to be less than the quoted error of our thresholds.[23]

For higher fragmentations the situation is quite different; decomposition rates must compete not only with the rate of extraction from the ion source but in addition with the higher rate of fragmentation in the decomposition channel with the lower threshold, and kinetic shifts may be substantial. This effect is apparent in the photoionization efficiency curves for the carbene fragments in Figures 3-5. The gradual onset makes identification of a threshold difficult and gives rise to the substantial uncertainties quoted in Table I for these processes.

Photoelectron spectra of $(CO)_5MnH$,[25] $(CO)_5MnCH_3$,[26] and $(CO)_5MnCF_3$[26] are reported in the literature. Adiabatic ionization potentials estimated from these data are also included in Table I for comparison to the PIMS results.

One concern is that the appearance potentials for the fragment ions do not occur at the thermodynamic threshold, but instead are determined by the onset of an available excited ion state.[27] Comparison of the fragment ion thresholds with available photoelectron spectra indicates this is not a complication.

The differences in the neutral bond energies, $D[(CO)_5Mn\text{-}R]$ calculated from the thresholds for appearance of $(CO)_5Mn^+$ are summarized in Table II.

The carbene bond energies, Table III, are derived from the thresholds for $(CO)_5Mn^+$ and $(CO)_5MnCXY^+$ in conjunction with the auxiliary thermochemical data given in Tables IV and V. An example of this calculation is given for $(CO)_5MnCH_2^+$ in Scheme I and summarized in eq. 3.

$$D[(CO)_5Mn^+\text{-}CH_2] = AP[(CO)_5Mn^+] - AP[(CO)_5MnCH_2^+] + D[CH_2\text{-}F] \quad (3)$$

Scheme I

$$\begin{array}{ccc} (CO)_5MnCH_2^+ + F & \xrightarrow{D[(CO)_5Mn^+\text{-}CH_2]} & (CO)_5Mn^+ + CH_2 + F \\ AP[(CO)_5MnCH_2^+] \downarrow & & \uparrow D(CH_2\text{-}F) \\ (CO)_5MnCH_2F & \xrightarrow[AP[(CO)_5Mn^+]]{} & (CO)_5Mn^+ + CH_2F \end{array}$$

The fluoride affinities of the carbenes, $D[(CO)_5MnCXY^+\text{-}F^-]$ are calculated from $AP[(CO)_5MnCXY^+]$and the electron affinity of F, 3.4 eV, according to eq. 4, and presented in Table III. The hydride affinities

$$D[(CO)_5MnCXY^+\text{-}F^-] = AP[(CO)_5MnCXY^+] - EA[F] \quad (4)$$

of the carbenes, $D[(CO)_5MnCXY^+ - H^-]$ are also given in Table III. These are calculated somewhat more indirectly; calculation of $D[(CO)_5MnCH_2^+\text{-}H^-]$ is given as an example in Figure 6.

Table II. Comparison of the Bond Energies $D[(CO)_5Mn\text{-}R]$

	$D[(CO)_5Mn\text{-}H] - D[(CO)_5Mn\text{-}R]$	$D[(CO)_5Mn\text{-}R]$	
Compound		This work[b]	Ref. 12
$(CO)_5MnH$	0	57	57
$(CO)_5MnCH_3$	13 ± 3	44	33
$(CO)_5MnCH_2F$	25 ± 3	32	
$(CO)_5MnCHF_2$	24 ± 3	33	
$(CO)_5MnCF_3$	15 ± 3	42	37

a) All data in kcal/mol at 298 K.

b) Assuming $D[(CO)_5Mn\text{-}H] = 57$ kcal/mol.[12]

Table III. Carbene Bond Energies and the Fluoride and Hydride Affinities of the Carbene Ions[a)]

Ion	$D[(CO)_5Mn^+-CXY]$	$D[(CO)_5MnCXY^+-F^-]$	$D[(CO)_5MnCXY^+-H^-]$
$(CO)_5MnCH_2^+$	104 ± 3	146 ± 3	214 ± 5
$(CO)_5MnCHF^+$	98 ± 10	145 ± 3	184 ± 5
$(CO)_5MnCF_2^+$	82 ± 3	150 ± 3	182 ± 5

a) All values in kcal/mol at 298 K.

Table IV. Thermochemical Properties of Methane and the Fluoromethanes.[a,b]

R	$\Delta H_f^\circ(R)$	$\Delta H_f^\circ(RH)$	$\Delta H_f^\circ(RF)$	D(R-H)	D(R-F)	$D(R^+-H^-)$	$D(R^+-F^-)$
CH_3	34.0	-17.89	-55.9	104.0	108.6	312.2	255.5
CH_2F	-4.9	-55.9	-108.1	103.1	121.9	289.6	247.1
CHF_2	-59.2	-108.1	-166.3	101.0	125.8	283.9	247.4
CF_3	-112.2	-166.3	-223.0	106.2	129.5	299.0	260.0

a. All values in kcal/mol at 298 K.

b. All data from the selected values in Ref. 31; error limits are typically ± 1 kcal/mol.

Table V. Summary of Additional Thermochemical Data Used in this Study[a]

Species	ΔH_f°	Reference
CH_2	92.4	b
CHF	30 ± 7	c
CF_2	-44.0 ± 1.0	d
F	18.9	c
H	52.09	c
CH_2CH_2	12.54	c
CH_2CF_2	-82.5 ± 2.4	e
CF_2CF_2	-157.4 ± 0.7	c
HCO	6.7 ± 1.3	f
CH_3CO	-5.4	g
CO	-26.42	c
C_2H_5	25.7	h
EA(F)	3.40 eV	i
EA(H)	0.754 eV	j

a. All values in kcal/mol at 298 K except as noted.

b. Chase, M. W.; Curnett, J. L.; Prophet, H.; McDonald, R. A.; Syverud, A. N. J. Phys. Chem. Ref. Data, Suppl. 1975, 4, No.1.

c. Stull, D. R.; Prophet, H. Natl. Stand. Ref. Data Ser., Natl. Bur. Stand. 1971, No. 37.

d. Schug, K. P.; Wagner, H. G. Ber. Bunsenges, Phys. Chem. 1978, 82, 719.

e. Lacher, J. R.; Skinner, H. A. J. Chem. Soc. A, 1968, 1034.

Table V. footnotes continued.

---

f. Dyke, J. M.; Jonathan, N. B. H.; Morris, A.; Winter, M. J. Molec. Phys. 1980, 39, 629.

g. Golden, D. M.; Benson, S. W. Chem. Rev. 1969, 69, 125.

h. Kerr, J. A. Chem. Rev. 1966, 66, 465.

i. Milstein, R.; Berry, R. S. J. Chem. Phys. 1971, 55, 4146.

j. Wagman, D. D.; Evans, W. H.; Parker, V. B.; Halow, I.; Bailey, S. M.; Schumm, R. H. Natl. Bur. Stand. Tech Note 270-3 1968.

FIGURE 6. Summary of the reactions from which $D[(CO)_5MnCH_2^+-H^-]$ is calculated.

$(CO)_5MnCH_2F \rightarrow (CO)_5MnCH_2^+ + F + e \quad AP[(CO)_5MnCH_2^+]$

$(CO)_5MnCH_3 \rightarrow (CO)_5Mn^+ + CH_3 + e \quad AP_1[(CO)_5Mn^+]$

$(CO)_5Mn^+ + CH_2F + e \rightarrow (CO)_5MnCH_2F \quad -AP_2[(CO)_5Mn^+]$

$CH_3 + F \rightarrow CH_3F \quad -D[CH_3\text{-}F]$

$CH_3F \rightarrow CH_2F + H \quad D[CH_2F\text{-}H]$

$H + e \rightarrow H^- \quad -EA[H]$

$(CO)_5MnCH_3 \rightarrow (CO)_5MnCH_2^+ + H^- \quad D[(CO)_5MnCH_2^+ - H^-]$

$$D[(CO)_5MnCH_2^+\text{-}H^-] = AP[(CO)_5MnCH_2^+] + AP_1[(CO)_5Mn^+] - AP_2[(CO)_5Mn^+] - D[CH_3\text{-}F] + D[CH_2F\text{-}H] - EA[H]$$

Fluoride and Hydride Transfer Reactions. $(CO)_5MnCH_3$ does not produce $(CO)_5MnCH_2^+$ either by electron impact, reaction with proton donors, or reaction with fragments produced by electron impact of $(CO)_5MnCH_3$ or $(CO)_5MnH$, even though $D[(CO)_5MnCH_2^+-H^-] = 210$ kcal/mol is so low as to indicate hydride abstraction is thermodynamically favorable.

The fluoroalkyl derivatives all give a $(CO)_5MnCXY^+$ carbene produced by F atom loss as a major fragment in the electron impact mass spectrum. In addition, F^- abstraction by a variety of the fragment ions (e.g., Mn^+, MnF^+, and often $(CO)_5Mn^+$) also produces the carbenes. This enables the fluoride and hydride transfer reactions of each of these carbenes to be investigated.

Reactions 5 and 6 are identified in $(CO)_5MnCH_2F$ at a pressure of 5×10^{-7} torr. Variation of ion abundance with time is illustrated in Figure 7; rate constants $k_5 = 3.3 \times 10^{-10}$ cm^3 molec^{-1} s^{-1} and

$$(CO)_5MnCH_2^+ + (CO)_5MnCH_2F \rightarrow (CO)_5MnCHF^+ + (CO)_5MnCH_3 \quad (5)$$

$$(CO)_5MnCHF^+ + (CO)_5MnCH_2F \rightarrow (CO)_5MnCF_2^+ + (CO)_5MnCH_3 \quad (6)$$

$k_6 = 1.7 \times 10^{-10}$ cm^3 molec^{-1} s^{-1} are derived from these data. Reaction 6 cannot be described simply as a hydride or fluoride transfer reaction; presumably an intermediate is formed which disproportionates as shown in Scheme II.

The carbene $(CO)_5MnCHF^+$ is not observed to react with $(CO)_5MnCHF_2$ at 5×10^{-7} torr of the neutral and at trapping times as long as 2000 msec.

FIGURE 7. Variation of the carbene ion abundances with time, observed in 5×10^{-7} torr $(CO)_5MnCH_2F$ following a 10 msec, 18 eV electron beam pulse.

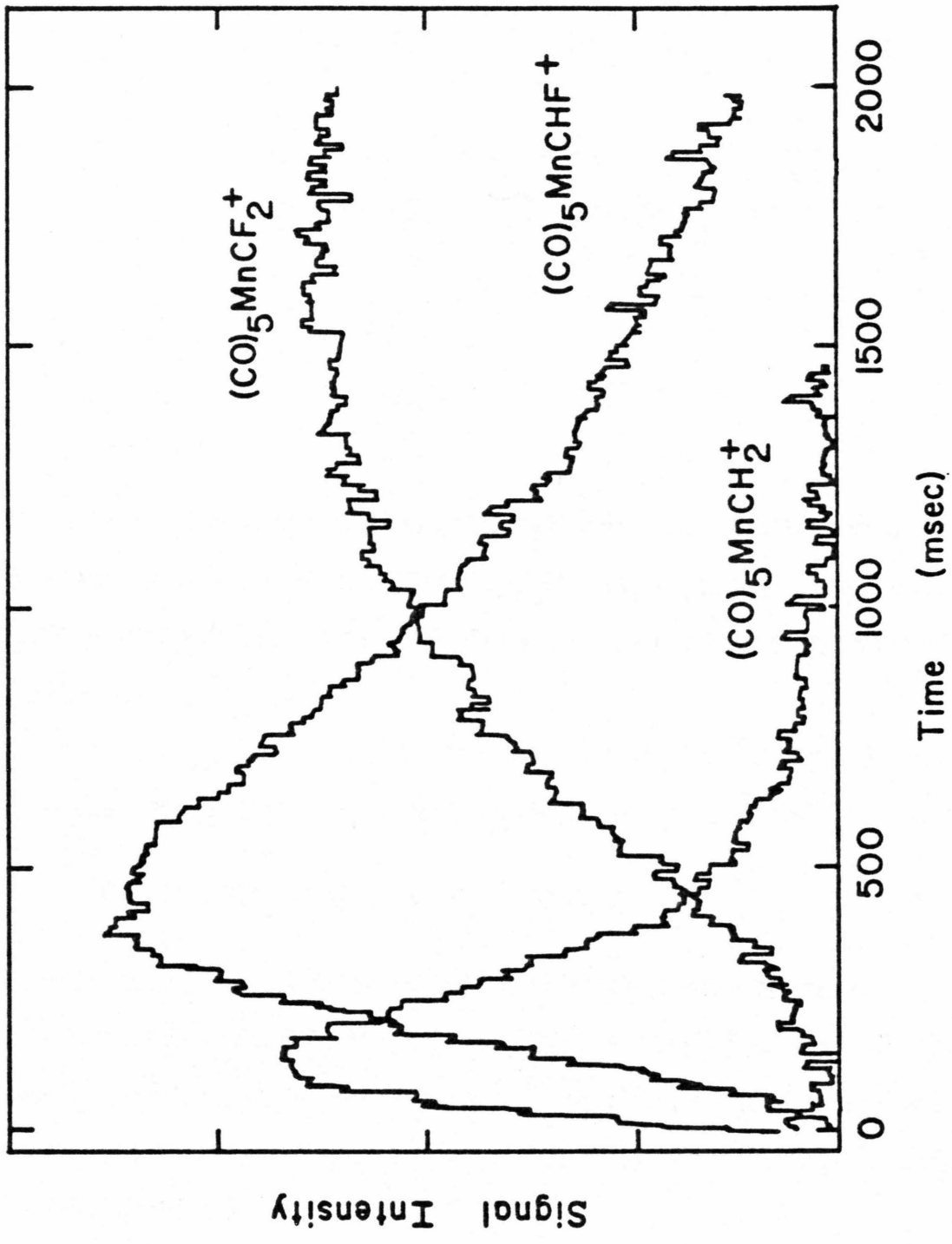
$(CO)_5MnCF_2^+$
$(CO)_5MnCHF^+$
$(CO)_5MnCH_2^+$
0
500
1000
1500
2000
Time (msec)
Signal Intensity

Scheme II

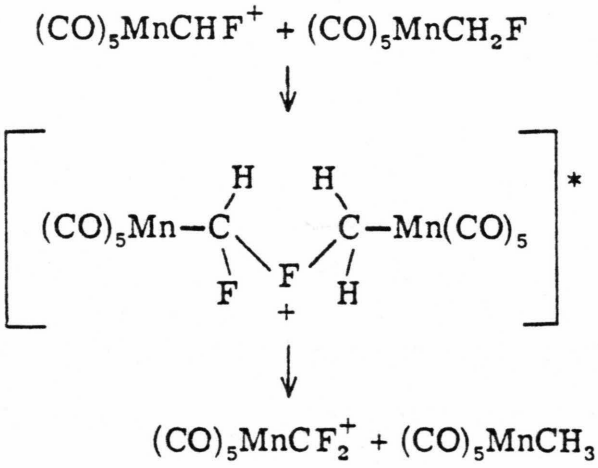

In a 1:1 mixture of $(CO)_5MnCH_2F$ with $(CO)_5MnCHF_2$ at a total pressure of 1×10^{-6} torr, $(CO)_5MnCHF^+$ is not observed to react with $(CO)_5MnCH_2F$ (to produce $(CO)_5MnCH_2^+$), even at trapping times up to 2000 msec.

In a 1:1 mixture of $(CO)_5MnCH_2F$ with $(CO)_5MnCF_3$ at a total pressure of 1×10^{-6} torr, the fluoride transfer reaction 7 is identified.

$$(CO)_5MnCH_2^+ + (CO)_5MnCF_3 \rightarrow (CO)_5MnCF_2^+ + (CO)_5MnCH_2F \qquad (7)$$

Careful examination of the double resonance contributions to $(CO)_5MnCF_2^+$ from $(CO)_5MnCH_2^+$ and $(CO)_5MnCHF^+$ indicate the direct reaction 7 and not just the sequential reactions 5 and 6 occur in this system. The complexity of the reaction scheme made it difficult to determine k_7.

Figure 8 illustrates the variation of ion abundances for $(CO)_5MnCHF^+$ and $(CO)_5MnCF_2^+$ formed in a 3:4 mixture of $(CO)_5MnCHF_2$ and $(CO)_5MnCF_3$ at a total presure of 2.5×10^{-7} torr. Although it appears

FIGURE 8. Variation of the carbene ion abundances with time, observed in a 3:4 mixture of $(CO)_5MnCHF_2$ with $(CO)_5MnCF_3$ at a total pressure of 2.5×10^{-7} torr, following a 10 msec, 18 eV electron beam pulse.

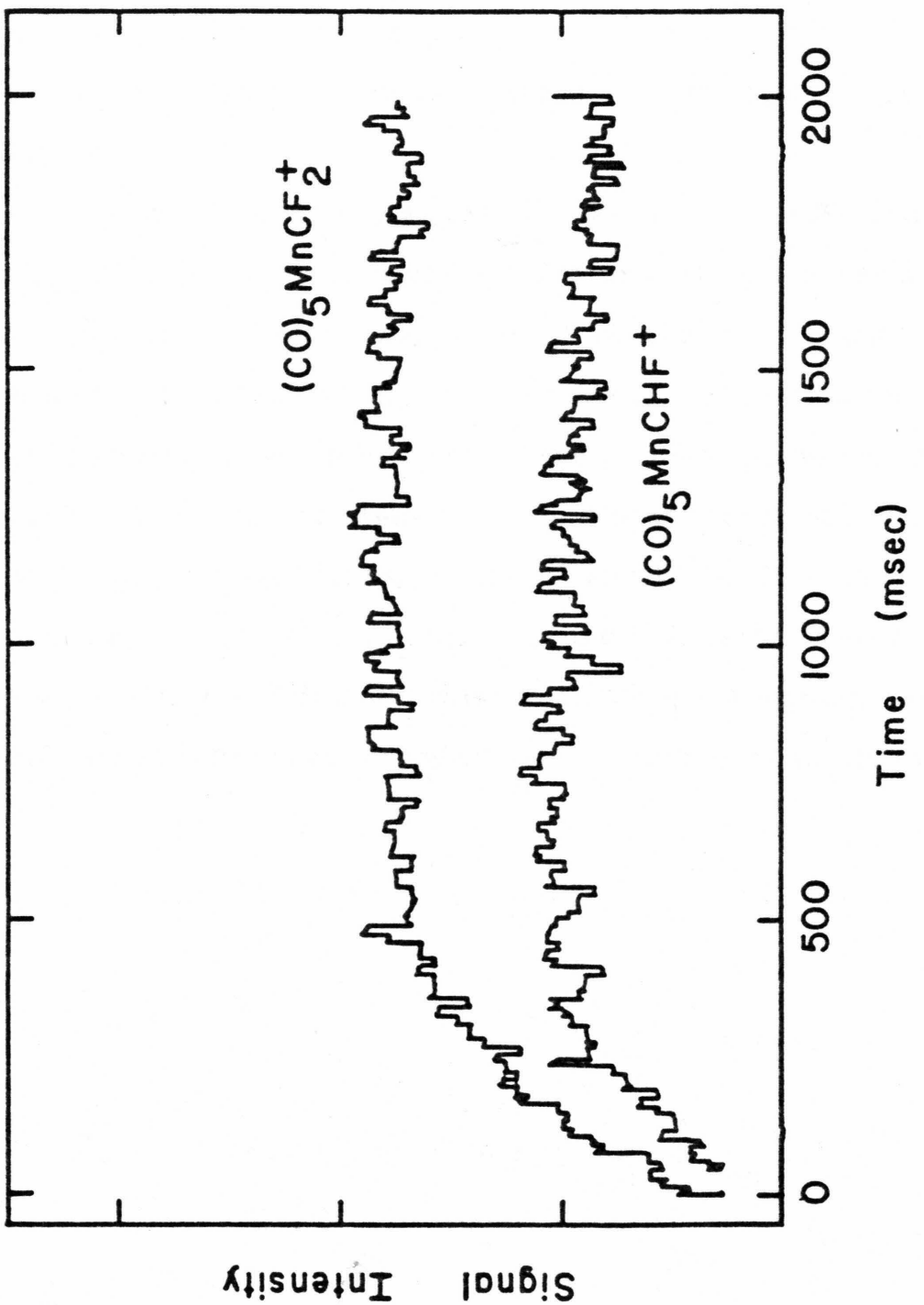
Signal Intensity
0
500
1000
1500
2000
Time (msec)
$(CO)_5MnCF_2^+$
$(CO)_5MnCHF^+$

an equilibrium is established between these two ions, and the ion abundances vary with pressure as expected for an equilibrium, no reaction linking these two ions is identified in the double resonance spectrum.

In several instances, as the mixture of $(CO)_5MnCHF_2$ with $(CO)_5MnCF_3$, fluoride (or hydride) transfer must be exothermic for one combination of reactants, but is not observed. It might be argued that electrophilic attack occurs on the metal, not the fluorine, and this is responsible for the failure to observe fluoride transfer as a rapid process. However, reaction of proton donors with the fluoroalkyls results only in proton transfer with HF loss to yield the carbene ions. The conjugate acids $(CO)_5Mn(R)H^+$, or the loss of the fluoromethanes to yield $(CO)_5Mn^+$, which would indicate attack at the manganese or the alkyl carbon, are not observed by proton transfer of any exothermicity.

Discussion

Scheme III illustrates the thermodynamic cycle from which $IP[(CO)_5Mn]$ can be calculated. Choosing $D[(CO)_5Mn\text{-}H] = 57$ kcal/mol[12] and $AP[(CO)_5Mn^+] = 10.3$ eV when formed from $(CO)_5MnH$, (Table I) gives $IP[(CO)_5Mn] = 7.8$ eV. The higher value

Scheme III

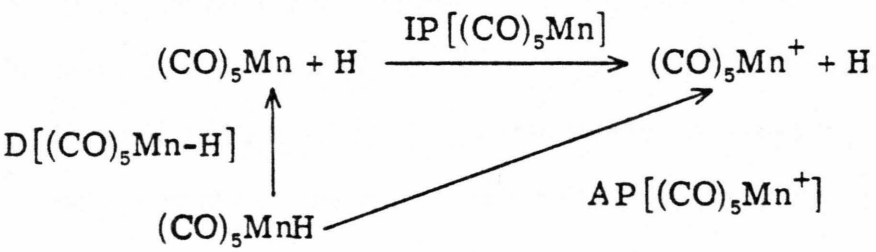

$D[(CO)_5Mn - H] = 64$ kcal/mol[14] yields $IP[(CO)_5Mn] = 7.5$ eV. A mass spectrometric determination of $IP[(CO)_5Mn] = 8.32$ eV is reported; a value for $IP[(CO)_{10}Mn_2] = 8.46$ is given by the same authors.[28] A value for the adiabatic $IP[(CO)_{10}Mn_2] = 7.7 \pm 0.1$ eV is found from the published photoelectron spectrum,[29] from which we estimate $IP[(CO)_5Mn] \cong 7.55 \pm 0.1$ eV by comparison to the mass spectral study. This is in reasonable agreement with the predictions based upon the manganese-hydrogen bond energies given above. A value $D[(CO)_5Mn\text{-}H] = 57$ kcal/mol is chosen as the reference point in this work.

The value for $D[(CO)_5Mn\text{-}H] = 57$ kcal/mol is used to calculate $D[(CO)_5Mn\text{-}R]$ of 44 kcal/mol ($R = CH_3$), 32 kcal/mol ($R = CH_2F$), 33 kcal/mol ($R = CHF_2$), and 42 kcal/mol ($R = CF_3$). The metal-

hydrogen bond is considerably stronger than the metal-methyl bond in these complexes. This is consistent with other thermochemical data, listed in Table VI, which provide a comparison of metal-methyl and metal-hydrogen bond strengths.

The bond strengths for the fluoroalkyls roughly follow the trends in D[R-H] for the fluoromethanes (Table IV): the bonds to CH_2F and CHF_2 are weaker than those to CH_3 and CF_3. Within our error limits, the manganese-methyl and -trifluoromethyl bonds are the same strength. What is striking about the $(CO)_5Mn$-R bond strength is the magnitude of these differences (12 kcal/mol), particularly considering the absolute bond energies of the manganese-carbon bonds are a factor of two or three smaller than in the fluoromethane. Even more startling, the metal-fluoroalkyls bonds are <u>weaker</u> than the manganese-methyl bond. This is in complete contrast to <u>all</u> the predictions based upon spectral evidence and kinetic reactivities of these complexes. A combination of weaker sigma-bonding and increased pi-bonding may account for some of the spectral changes occurring with fluorine substitution. Activation parameters, thermochemical properties of final products, and availability of reaction pathways apparently play the major roles in determining the thermal "stability" of the fluorocarbon derivatives.

Comparison of the bond energies derived in the present work to those reported by Connor (Table II) reveals only partial agreement. For R = CF_3, the results differ by only 1 kcal/mol. The euphoria fades in the case of R = CH_3, where Connor's bond energy is 11 kcal/mol below our number. This discrepancy is larger than the

Table VI. Comparison of Metal-Hydrogen and Metal-Methyl Bond Strengths[a]

Compound, MR	$D[M-H] - D[M-CH_3]$	$D[M-H]$
$(\eta^5\text{-}C_5H_5)_2MoR_2$[b]	24.5 ± 1.5 (mean)	60 (est.)
$(\eta^5\text{-}C_5H_5)_2WR_2$[b]	25.4 ± 1.4 (mean)	73 (est.)
$IrCl(CO)(PMe_3)_2(I)(R)$[c]	13.6 ± 3	
CoR[d]	-2 ± 12	39 ± 6

a) All values in kcal/mol at 298 K.

b) Ref. 10.

c) Ref. 11.

d) Ref. 15.

error limits which might reasonably be expected for either method. It would be improbable that the threshold for formation of $(CO)_5Mn^+$ from $(CO)_5MnCH_3$ is 0.5 eV lower than indicated by the data in Figure 2. Some problems were noted by Connor in applying the drop calorimetry method for determining heats of iodination to the methyl derivative.[12]

The knowledge that the double bond energy in tetrafluoroethylene is 60 kcal/mol less than ethylene makes the observed weakening of metal carbene bond energies by successive fluorine substitution less surprising. The effect is non-trivial, with $D[(CO)_5Mn^+-CH_2] = 104$, $D[(CO)_5Mn^+-CHF] = 98$, and $D[(CO)_5Mn^+-CF_2] = 82$ kcal/mol. These are compared to fluorine substituent effects on "bare" metal-carbene bond energies in Table VII, where a similar weakening of the bond is effected by fluorine substitution.

A weak bond does not necessarily imply lack of stability. Even though the CF_2 carbene has the weakest bond to $(CO)_5Mn^+$, it is the final product of hydride and fluoride transfer reactions 5 and 6 observed in $(CO)_5MnCH_2F$. Similar hydride transfers have been observed for cationic rhenium and iron methylene complexes reacting with their methoxymethyl precursors.[30,31] The formation of $(CO)_5MnCF_2^+$ by reaction 6 in the presence of $(CO)_5MnCH_2F$ is interesting. The fluoride transfer to yield $(CO)_5MnCH_2^+$ (which would provide a chain reaction producing $(CO)_5MnCH_3$ and $(CO)_5MnCHF_2$ from $(CO)_5MnCH_2F$) is calculated (Table III) to be 1 kcal/mol endothermic; it does not occur. The overall exchange reaction 6 is calculated to be 31 kcal/mol exothermic.

Table VII. Metal-Carbene Bond Energies to Transition Metal Ions[a]

Metal ion, M^+	$D[M^+-CH_2]$	$D[M^+-CF_2]$
Mn^+	98 ± 6[b, c]	
Ni^+	86 ± 6[b]	44 ± 5[b]

a) All values in kcal/mol at 298 K.

b) Halle, L. F.; Beauchamp, J. L., unpublished data.

c) Stevens, A. E.; Beauchamp, J. L. J. Am. Chem. Soc. 1979, 101, 6449.

Several of the hydride and fluoride transfers are too slow ($k < 10^{-12}$ cm^3 molec^{-1} s^{-1}) to be observed on the icr time scale, as the studies with the mixture of $(CO)_5MnCHF_2$ and $(CO)_5MnCF_3$ highlight. Fluoride transfer in this system is nearly thermoneutral; this may account for the slowness of the reaction. Since hydride transfers to and from several of these carbenes are facile, it does not appear that steric effects are important. Failure to observe the fluoride transfer reactions may be due to unfavorable energetics associated with fluoronium ion intermediates with several fluorine substituents on the α-carbons. This effect has been noted in a study of the fluoromethanes.[32]

Both the hydride and fluoride affinities of the carbenes follow the trends observed for the fluoroalkanes, but are substantially (100 kcal/mol) weaker. These considerations indicate the carbenes should <u>not</u> be regarded as carbonium ions, but that the positive charge is likely to be on the metal. This reduced charge on the carbene carbon could also be a factor contributing to the slow hydride and fluoride transfer rates.

The hydride and fluoride transfers observed in the icr experiments establish $D[(CO)_5MnCH_2^+ - H^-] > D[(CO)_5MnCHF^+-H^-]$, in agreement with the PIMS data. The reactions indicate $D[(CO)_5MnCH_2^+-F^-] > D[(CO)_5MnCF_2^+-F^-]$, which is the reverse of that predicted from the PIMS data. The gradual onset for the carbene ions makes the thresholds difficult to assign; a reversal of these two fluoride affinities falls within the error limits placed on these appearance potentials.

The thermochemical data in this work can be used to predict the enthalpy changes for several reactions, listed in Table VIII.

One interesting reaction is the insertion of CO into the $(CO)_5Mn$-R bond. The enthalpy change $\Delta H = -12.6$ kcal/mol for insertion of CO into the methyl compound is reported,[2] from which $D[(CO)_5Mn\text{-}C(O)CH_3] = 44$ kcal/mol can be derived. In calculating ΔH for the other insertion reactions in Table VIII, the manganese-formyl and manganese-fluoroacyl bonds were assumed equal to 44 kcal/mol also; increasing the bond energy for these complexes increases the exothermicity of CO insertion.

The approximately 6 kcal/mol exothermicity of CO insertion to yield the formyl, $(CO)_5MnC(O)H$ indicates that the rapid decomposition of this compound should not be attributed entirely to thermodynamic instability. A trend as predicted for the fluoroalkyls is consistent with that determined experimentally for a series of iridium compounds.[22]

One reaction common to a variety of metal alkyls is β-hydrogen transfer to yield a metal hydride and a free olefin. An estimate for the endothermicity of this decomposition for $(CO)_5MnCH_2CH_3$ can be made by assuming $D[(CO)_5Mn\text{-}CH_2CH_3]$ is equal to $D[(CO)_5Mn\text{-}CH_3]$; this is given in Table VIII. Not surprisingly, $(CO)_5MnCH_2CH_3$ is an isolable species. This complex is thermally unstable above 60°, but decomposes to yield products other than the hydride.[33]

The enthalpies for metathesis reactions of the $(CO)_5MnCH_2^+$ and $(CO)_5MnCF_2^+$ carbenes are also examined in Table VIII. Although the $(CO)_5Mn^+\text{-}CF_2$ bond is weakest, the carbon-carbon bonds in the olefins are the dominating factor in these reactions: the $(CO)_5MnCF_2^+$ carbene

Table VIII. Reaction Enthalpies Calculated From This Work

Reaction	ΔH kcal/mol
CO Insertion	
$(CO)_5MnCH_3 + CO \rightarrow (CO)_5MnC(O)CH_3$	-12.6[a]
$(CO)_5MnH + CO \rightarrow (CO)_5MnC(O)H$	-6
$(CO)_5MnCH_2F + CO \rightarrow (CO)_5MnC(O)CH_2F$	-25
$(CO)_5MnCHF_2 + CO \rightarrow (CO)_5MnC(O)CHF_2$	-24
$(CO)_5MnCF_3 + CO \rightarrow (CO)_5MnC(O)CF_3$	-15
β-Hydrogen Transfer	
$(CO)_5MnCH_2CH_3 \rightarrow (CO)_5MnH + CH_2CH_2$	26
Olefin Metathesis	
$(CO)_5MnCH_2^+ + CF_2CF_2 \rightarrow (CO)_5MnCF_2^+ + CH_2CF_2$	-40
$(CO)_5MnCH_2^+ + CH_2CF_2 \rightarrow (CO)_5MnCF_2^+ + CH_2CH_2$	-19

a. From Ref. 2.

is thus favored. These results again suggest caution should be exercised in evaluating "stabilities" of organometallic complexes without regard for the other reactants and products. Metathesis reactions have not been examined with either fluorocarbenes or fluoro-olefins; these would make an interesting test of our predictions.[34]

Acknowledgments

The Caltech-JPL PIMS facility was made possible by a grant from the President's Fund of the California Institute of Technology. We thank Dr. M.-T. Leu of the Jet Propulsion Laboratory for his generous loan of the electronics for the quadrupole mass-spectrometer. This work was supported in part by the United States Department of Energy.

References and Notes

1. Stone, F. G. A. Endeavor 1966, 25, 33. Treichel, P. M.; Stone, F. G. A. Advan. Organomet. Chem. 1964, 1, 143.
2. Calderazzo, F. Angew. Chem. Int. Ed. Engl. 1977, 16, 299.
3. Noack, K.; Schaerer, U.; Calderazzo, F. J. Organomet. Chem. 1967, 8, 517.
4. King, R. B. "Organometallic Syntheses, Vol. 1," Academic Press: New York, 1965.
5. Fiato, R. A.; Vidal, J. L.; Pruett, R. L. J. Organomet. Chem. 1979, 172, C4.
6. Cotton, F. A.; Wing, R. M. J. Organomet. Chem. 1967, 9, 511.
7. Bennett, M. A.; Chee, H.-K.; Robertson, G. B. Inorg. Chem. 1979, 18, 1061, and references therein. Bennett, M. A.; Chee, H.-K.; Jeffery, J. C.; Robertson, G. B. Inorg. Chem. 1979, 18, 1071.
8. Cotton, F. A.; Lukehart, C. M. Prog. Inorg. Chem. 1972, 16, 487. Block, T. F.; Fenske, R. F. J. Am. Chem. Soc. 1977, 99, 4321, and references therein.
9. Connor, J. A. Top. Curr. Chem. 1977, 71, 71, and references therein.
10. Calado, J. C. G.; Dias, A. R.; Martinho-Simoes, J. A.; Ribeiro da Silva, M. A. V. J. Organomet. Chem. 1979, 174, 77.
11. Yoneda, G.; Blake, D. M. J. Organomet. Chem. 1980, 190, C71.

References (continued)

12. Connor, J. A., private communication; preliminary results for $(CO)_5MnCH_3$ are given in Brown, D. L. S.; Connor, J. A.; Skinner, H. A. J. Organomet. Chem. 1974, 81, 403.

13. Halpern, J.; Ng, F. T. T.; Rempel, G. L. J. Am. Chem. Soc. 1979, 101, 7124.

14. Halpern, J., private communication, based on data reported in Sweany, R. L.; Halpern, J. J. Am. Chem. Soc. 1977, 99, 8335.

15. Armentrout, P. B.; Beauchamp, J. L. J. Am. Chem. Soc. 1980, 102, 1736.

16. Stevens, A. E.; Beauchamp, J. L. J. Am. Chem. Soc., to be submitted.

17. Distefano, G. J. Res. Natl. Bur. Stand., Sect. A. 1970, 74, 233, and references therein.

18. LeBreton, P. R.; Williamson, A. D.; Beauchamp, J. L.; Huntress, W. T. J. Chem. Phys. 1975, 62, 1623.

19. Beauchamp, J. L. Annu. Rev. Phys. Chem. 1971, 22, 527. McMahon, T. B.; Beauchamp, J. L. Rev. Sci. Instr. 1972, 43, 509.

20. Davison, A.; Faller, J. W. Inorg. Chem. 1967, 6, 845.

21. Clossen, R. D.; Kozikowski, J.; Coffield, T. H. J. Org. Chem. 1957, 22, 598. Hieber, W.; Wagner, G. Justus Liebigs Ann. Chem. 1958, 618, 24.

22. Blake, D. M.; Winkelman, A.; Chung, Y. L. Inorg. Chem. 1975, 14, 1326.

References (continued)

23. Vestal, M. L., in Ausloos, P., Ed., "Fundamental Processes in Radiation Chemistry", Wiley: New York, 1968.

24. Chupka, W. A. J. Chem. Phys. 1971, 54, 1936.

25. Hall, M. B. J. Am. Chem. Soc. 1975, 97, 2057.

26. Lichtenberger, D. L.; Fenske, R. F. Inorg. Chem. 1974, 13, 486.

27. This phenomenon is well known; examples can be found in Baer, T.; Werner, P. S.; Tsai, B. P.; Lin, S. F. J. Chem. Phys. 1974, 61, 5468.

28. Junk, G. A.; Svec, H. J. J. Chem. Soc. (A) 1970, 2102.

29. Higginson, B. R.; Lloyd, D. R.; Evans, S.; Orchard, A. F. J. Chem. Soc., Faraday Trans. 2 1975, 71, 1913.

30. Stevens, A. E.; Beauchamp, J. L. J. Am. Chem. Soc. 1978, 100, 2584.

31. Wong, W.-K.; Tam, W.; Gladysz, J. A. J. Am. Chem. Soc. 1979, 101, 5440.

32. Blint, R. J.; McMahon, T. B.; Beauchamp, J. L. J. Am. Chem. Soc. 1974, 96, 1269.

33. Green, M. L. H.; Nagy, P. L. I. J. Organomet. Chem. 1963, 1, 58.

34. Several cationic molybdenum perfluorocarbene complexes have been prepared: Reger, D. L.; Dukes, M. D. J. Organomet. Chem. 1978, 153, 67.

Chapter V

Metal-Hydrogen Bond Energies in Protonated Transition Metal Complexes

Metal-Hydrogen Bond Energies in Protonated Transition Metal Complexes.

Sir:

Existing data for transition metal-hydrogen bond dissociation energies of neutral complexes are few and controversial[1-8]. For the ion BH^+, the homolytic bond energy $D(B^+-H)$ can be determined readily and accurately from the proton affinity (PA) and adiabatic ionization potential (IP) of the base B, as shown in the thermodynamic cycle of Scheme I, which yields the relationship given in eq 1.

Scheme I

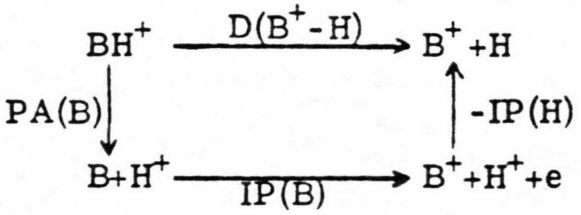

$$D(B^+-H) = PA(B) + IP(B) - IP(H) \qquad (1)$$

We report the proton affinities of twenty organotransition metal complexes in the gas phase. For sixteen of these complexes protonation occurs on the metal center, and the corresponding metal-hydrogen homolytic bond dissociation energies are determined. These data are summarized in Table I.

All proton affinities were determined using the techniques of ion cyclotron resonance spectroscopy[9], by examining proton transfer reactions in mixtures with compounds of known base strength. Ionization potentials are taken from a variety of sources and experimental procedures, as noted in Table I. The site of protonation in several of these

Table I. Proton affinities, ionization potentials, and metal-hydrogen homolytic bond energies of transition metal compounds.

Compound (B)	PA(B)-PA(NH_3)[a] kcal/mol	PA(B)[b] kcal/mol	Adiabatic IP(B)[a, c] eV	Homolytic Bond Energy D[B^+-H] kcal/mol	Site of[a, d] Protonation
		Group VB			
$(CO)_6V$	-9.7±1.3	197±3	7.45±0.1(PES)[k]	56±3	
		Group VIB			
$(CO)_6Cr$	-23.3±1.1	184±2	8.142±0.017(PIMS)[l]	58±3	
$(CO)_6Mo$	-18±1	189±2	8.227±0.011(PIMS)[l]	65±3	
$(CO)_6W$	-19±1	188±2	8.242±0.006(PIMS)[l]	64±3	
$CpCr(CO)_2NO$	-7.2±1.3	200±2	7.2±0.1(PES)[m]	52±3	L(g)
$CpCr(CO)_3CH_3$	1.8±1.8	209±3	7.2±0.2(ICR)	61±4	L(g)
$BzCr(CO)_3$	1±2	208±3	7.0±0.1(PES)[n]	56±4	M(s)[u]
		Group VIIB			
$(CO)_5MnCH_3$	-18.7±1.4[e]	188±3	8.3±0.1(PES)[o]	67±3	
$(CO)_5ReCH_3$	-16.3±1.0[e]	191±2	8.5±0.1(PES)[p]	73±3	
$(CO)_5MnH$	-3.5±1.5	204±3	8.55±0.1(PES)[p]	87±3	
$(CH_3C_5H_4)Mn(CO)_3$	-3.9±0.2[f]	203±2	7.86±0.1(MS)[q]	71±3	M(s)[v]
		Group VIII			
$(CO)_5Fe$	-3±3[g]	204±4	7.98±0.01(PIMS)[r]	74±5	M(s)[u]
$CpFe(CO)_2CH_3$	-13.3±1.1	194±2	7.5±0.1(PES)[s]	53±3	
Cp_2Fe	6±4[h]	213±5	6.72±0.1(PES)[t]	54±5	M(s)[x]
Cp_2Ru	13±2	220±3	7.5±0.2(ICR)	79±5	M(s)[x, y]
$CpCo(CO)_2$	0±2	207±3	7.8±0.2(ICR)	73±5	M(g)
$CpRh(CO)_2$	7±2	214±3	7.8±0.2(ICR)	80±5	M(g)
$(CO)_4Ni$	-23±1	184±2	8.32±0.01(PIMS)[r]	62±3	
Cp_2Ni	17.9±1[i]	225±3	6.2±0.1(PES)[t]	54±3	L(s)[z]
$CpNiNO$	-4.5±2.5[j]	203±3	8.21±0.03(PIMS)[j]	78±3	L(g)[j]

Table I References

a. All references are from this work unless otherwise noted.

b. Relative to PA(NH_3) = 207±2 kcal/mol. Although PA(NH_3) remains controversial, lower and upper limits of 204 and 208 kcal/mol seem well established [Houle, F. A.; Beauchamp, J. L. J. Am. Chem. Soc. 1979, 101, 4067]. A lower value of PA(NH_3) would result in lowering all of the homolytic bond dissociation energies by the same amount.

c. The technique used for determination is indicated in parentheses: Photoelectron spectroscopy (PES), photoionization spectroscopy (PIMS), or mass spectroscopy (MS). Those IP denoted ICR were determined by the extrapolated voltage difference method [Warren, J. W. Nature 1950, 165, 810] on our instrument.

d. Metal protonation denoted by M, ligand by L, with subscripts referring either to solution-phase (s) or gas-phase (g) studies. Compounds for which no reference is given are assumed to protonate on the metal.

e. Stevens, A. E.; Beauchamp, J. L. J. Am. Chem. Soc. 1979, 101, 245.

f. Fernando, J.; Faigle, G.; Ferreira, A. M. da C.; Galembeck, S. E.; Riveros, J. M. J. Chem. Soc., Chem. Commun. 1978, 126.

g. Foster, M. S.; Beauchamp, J. L. J. Am. Chem. Soc. 1975, 97, 4808.

h. Foster, M. S.; Beauchamp, J. L. J. Am. Chem. Soc. 1975, 97, 4814.

i. Corderman, R. R.; Beauchamp, J. L. Inorg. Chem. 1976, 15, 665.

j. Corderman, R. R., Ph. D. Thesis, California Institute of Technology, 1977.

k. Evans, S.; Green, J. C.; Orchard, A. F.; Saito, T.; Turner, D. W.

Chem. Phys. Lett. 1969, 4, 361.

l. Lloyd, D. R.; Schlag, E. W. Inorg. Chem. 1969, 8, 2544.

m. Hubbard, J. L.; Lichtenberger, D. L. Inorg. Chem. 1980, 19, 1388.

n. Guest, M. F.; Hillier, I. H.; Higginson, B. R.; Lloyd, D. R. Molec. Phys. 1975, 29, 113.

o. Lichtenberger, D. L.; Fenske, R. F. Inorg. Chem. 1974, 13, 486.

p. Hall, M. B. J. Am. Chem. Soc. 1975, 97, 2057.

q. Efraty, A.; Huang, M. H. A.; Weston, C. A. Inorg. Chem. 1975, 14, 2796.

r. Distefano, G. J. Res. Natl. Bur. Stand., Sect. A 1970, 74, 233.

s. Lichtenberger, D. L.; Fenske, R. F. J. Am. Chem. Soc. 1976, 98, 50.

t. Rabalais, J. W.; Werme, L. O.; Bergmath, T.; Karlsson, L.; Hussain, M.; Seigbahn, K. J. Chem. Phys. 1972, 57, 1185.

u. Davison, A.; McFarlane, W.; Pratt, L.; Wilkinson, G. J. Chem. Soc. 1962, 3653.

v. This compound has not been studied; however, $(C_5H_5)Mn(CO)_3$[t], $(Et_4C_5H)Mn(CO)_3$[v] and $(Et_5C_5)Mn(CO)_3$[v] protonate at the metal.

w. Lokshin, B. V.; Ginzburg, A. G.; Setkina, V. N.; Kursanov, D.N.; Nemirovskaya, I. B. J. Organomet. Chem. 1972, 37, 347.

x. Curphey, T. J.; Santer, J. O.; Rosenblum, M.; Richards, J. H., J. Am. Chem. Soc. 1960, 82, 5249.

y. Cerichelli, G.; Illuminati, G.; Ortaggi, G.; Giuliani, A. M. J. Organomet. Chem. 1977, 127, 357.

z. Turner, G. K.; Kläui, W.; Scotti, M.; Werner, H.; J. Organomet. Chem. 1975, 102, C9.

compounds has been determined either by gas-phase or solution-phase studies; these results are also presented in Table I. For the cases indicated, ligand protonation corresponds to carbon-hydrogen, rather than metal-hydrogen bond formation.

The following points emerge from the data presented in Table I:

(1) An average metal-hydrogen bond energy of 68 kcal/mol is computed from the 16 compounds for which protonation on the metal center is indicated. The enormous range of energies, from 53 kcal/mol for $D[CpFe(CO)_2CH_3^+-H]$ to 87 kcal/mol for $D[(CO_5)MnH^+-H]$, would suggest this average should be used only with extreme caution to predict the thermochemistry or reactivity of metal hydrides.

(2) Despite the wide range of bond strengths, periodic trends are apparent. In moving across the first row transition metal carbonyls, the metal-hydrogen bond energy is a maximum for $D[(CO)_5Fe^+-H]$. On proceeding from a first-row compound to its second-row homologue, the metal-hydrogen bond energy increases. A difference of 7 kcal/mol is seen between $D[(CO)_6Cr^+-H]$ and $D[(CO)_6Mo^+-H]$, and between $D[CpCo(CO)_2^+-H]$ and $D[CpRh(CO)_2^+-H]$. A more substantial increase is evident with $D[Cp_2Ru^+-H]$, for which the bond energy is 25 kcal/mol stronger than $D[Cp_2Fe^+-H]$. There does not seem to be an increase in bond energy on proceeding from second to third row metals; the only example is $D[(CO)_6Mo^+-H]$ compared to $D[(CO)_6W^+-H]$, however. The 6 kcal/mol difference between $D[(CO)_5MnCH_3^+-H]$ and $D[(CO)_5ReCH_3^+-H]$ is consistent with these observations.

(3) Typically within a "homologous" series of compounds, the homolytic bond energy $D(B^+-H)$ remains constant.[11] It is clear on examining the three iron complexes listed in Table I that they do not

constitute "homologous" molecules. We suggest that compounds with higher oxidation states of the same metal atom have substantially weaker metal-hydrogen bonds. Forming several sigma bonds causes changes in the electron density and orbital hybridization of the metal center which result in weaker bonds with increasing oxidation state. This concept is not unfamiliar to most chemists; a Co(I)/Co(III) couple, but not a Co(III)/Co(V) couple, is prevalent in catalysis.

Connor[1] has also noted a decrease in bond energy with increasing oxidation state; he gives as an example the average metal-chlorine bond strengths in $MoCl_n$ and WCl_n, n = 4-6.

In this context, NO appears to have the same effect as a sigma-bonding ligand: protonation on the cyclopentadienyl ring, rather than on the metal, of the cyclopentadienyl chromium and nickel complexes is interpreted as evidence of a weaker metal-hydrogen bond for these compounds as well.

Although this hypothesis generally seems valid, an exception is $D[(CO)_5MnCH_3^+-H]$ = 67 kcal/mol compared to $D[(CO)_5MnH^+-H]$ = 87 kcal/mol; in this instance ligand variation has a striking effect on the bond strength.

(4) Although $D[(CO)_5MnH^+-H]$ is a very strong 87 kcal/mol, the second metal-hydrogen bond is very weak, reaction 2.

$$(CO)_5MnH_2^+ \xrightarrow{87\ \text{kcal/mol}} (CO)_5MnH^+ + H \xrightarrow{23\ \text{kcal/mol}} (CO)_5Mn^+ + 2H \quad (2)$$

These data give the reductive elimination of H_2 from $(CO)_5MnH_2^+$ 6 kcal/mol endothermic[10]. We expect this disparity between the first and second bond energies is a general result with dihydrides for which the unsaturated species (in this case $(CO)_5Mn^+$) has a singlet ground state.

(5) For main group hydrides the bond energy in the ion is typically 10-15 kcal/mol stronger than in the isoelectronic neutral.[11] The ions $(CO)_5FeH^+$ and $(CO)_4NiH^+$ are isoelectronic with $(CO)_5MnH$ and $(CO)_4CoH$, for which metal-hydrogen bond energies of 57[5]-64[4] and 55[6, 8]-58[7] kcal/mol have been estimated. For the transition metals the bond energies will depend heavily on the geometry and orbital hybridization at the metal. For example, $(CO)_4Ni^+$ is expected to be of nearly tetrahedral geometry, with the radical electron of predominantly d character. Although $(CO)_4Co$ may have a similar structure, several theoretical and experimental studies have suggested that $(CO)_4Co$ could be of C_{3v} geometry, with the radical electron of substantial s-p character.[12] These differences may cause changes in the bond energy between ion and neutral of such magnitude that comparisons or predictions between them are difficult to make at this point.

The principal objective in deriving the data presented in Table I is the determination of metal-hydrogen homolytic bond energies for a large number of organometallic complexes. The base strengths as well as other reactions observed with many of these species are also of interest. These will be discussed separately.

Acknowledgements

This work was supported in part by the United States Department of Energy. A. E. S. would like to thank N. S. F. for a Graduate Fellowship (1976-1979) during which time many of these data were determined.

Amy E. Stevens and J. L. Beauchamp*
Contribution No. 6264 from the Arthur Amos Noyes Laboratory of Chemical Physics,
California Institute of Technology,
Pasadena, California 91125
(Received)

References and Notes

1. Connor, J. A. Topics in Current Chemistry 1977, 71, 71, and references therein.
2. Yoneda, G.; Blake, D. M., J. Organomet. Chem. 1980, 190, C71.
3. Calado, J. C. G.; Dias, A. R.; Martinho Simões, J. A. J. Organomet. Chem. 1979, 174, 77.
4. Halpern, J., private communication, based upon data given in Sweany, R. L.; Halpern, J. J. Am. Chem. Soc. 1977, 99, 8335.
5. Connor, J. A., private communication.
6. Bronshtein, Yu. E.; Grankin, V. Yu.; Krinkin, D.P.; Rudkovskii, D. M. Russ. J. Phys. Chem. 1966, 40, 802.
7. Ungvary, F. J. Organomet. Chem. 1972, 36, 363.
8. Alemdaroğlu, N. H.; Penninger, J. M. L.; Oltay, E. Monatshefte 1976, 107, 1043.
9. Beauchamp, J. L. Annu. Rev. Phys. Chem. 1971, 22, 527.
10. Stevens, A. E.; Beauchamp, J. L., to be published.
11. Wolf, J. F.; Staley, R. H.; Koppel, I.; Taagepera, M.; McIver, Jr., R. T.; Beauchamp, J. L.; Taft, R. W. J. Am. Chem. Soc. 1977, 99, 5417.
12. Elian, M.; Hoffmann, R. Inorg. Chem. 1975, 14, 1058; Pensak, D. A.; McKinney, R. J. Inorg. Chem. 1979, 18, 3407, and references therein.

Abstract

The techniques of ion cyclotron resonance spectroscopy are used to determine the proton affinities of twenty organotransition metal complexes in the gas phase. Combined with adiabatic ionization potentials, these data yield metal-hydrogen homolytic bond energies for the sixteen species for which protonation occurs on the metal center. These bond energies range from 53 to 87 kcal/mol. Bond energies increase on going from a first-row complex to its second-row homologue, but no increase is seen on going to the third-row metal. The metal-hydrogen bond energy decreases markedly with increasing oxidation state of the same metal. Comparison to isoelectronic neutral complexes is made.